nanomaterials

MDPI

Review

Applications of Nanocellulose/Nanocarbon Composites: Focus on Biotechnology and Medicine

Lucie Bacakova [1,*], Julia Pajorova [1], Maria Tomkova [2], Roman Matejka [1], Antonin Broz [1], Jana Stepanovska [1], Simon Prazak [1], Anne Skogberg [3], Sanna Siljander [4] and Pasi Kallio [3]

1 Department of Biomaterials and Tissue Engineering, Institute of Physiology of the Czech Academy of Sciences, Videnska 1083, 14220 Prague, Czech Republic; Julia.Pajorova@fgu.cas.cz (J.P.); Roman.Matejka@fgu.cas.cz (R.M.); Antonin.Broz@fgu.cas.cz (A.B.); Jana.Stepanovska@fgu.cas.cz (J.S.); Simon.Prazak@fgu.cas.cz (S.P.)

2 Faculty of Biotechnology and Food Sciences, Slovak University of Agriculture in Nitra, Tr. A. Hlinku 2, 94976 Nitra, Slovakia; xtomkovam2@uniag.sk

3 BioMediTech Institute and Faculty of Medicine and Health Technology, Tampere University, Korkeakoulunkatu 3, 33014 Tampere, Finland; anne.skogberg@tuni.fi (A.S.); pasi.kallio@tuni.fi (P.K.)

4 Automation Technology and Mechanical Engineering, Faculty of Engineering and Natural Sciences, Tampere University, Korkeakoulunkatu 6, 33720 Tampere, Finland; sanna.siljander@tuni.fi

* Correspondence: Lucie.Bacakova@fgu.cas.cz; Tel.: +420-2-9644-3743

Received: 27 December 2019; Accepted: 21 January 2020; Published: 23 January 2020

Abstract: Nanocellulose/nanocarbon composites are newly emerging smart hybrid materials containing cellulose nanoparticles, such as nanofibrils and nanocrystals, and carbon nanoparticles, such as "classical" carbon allotropes (fullerenes, graphene, nanotubes and nanodiamonds), or other carbon nanostructures (carbon nanofibers, carbon quantum dots, activated carbon and carbon black). The nanocellulose component acts as a dispersing agent and homogeneously distributes the carbon nanoparticles in an aqueous environment. Nanocellulose/nanocarbon composites can be prepared with many advantageous properties, such as high mechanical strength, flexibility, stretchability, tunable thermal and electrical conductivity, tunable optical transparency, photodynamic and photothermal activity, nanoporous character and high adsorption capacity. They are therefore promising for a wide range of industrial applications, such as energy generation, storage and conversion, water purification, food packaging, construction of fire retardants and shape memory devices. They also hold great promise for biomedical applications, such as radical scavenging, photodynamic and photothermal therapy of tumors and microbial infections, drug delivery, biosensorics, isolation of various biomolecules, electrical stimulation of damaged tissues (e.g., cardiac, neural), neural and bone tissue engineering, engineering of blood vessels and advanced wound dressing, e.g., with antimicrobial and antitumor activity. However, the potential cytotoxicity and immunogenicity of the composites and their components must also be taken into account.

Keywords: nanofibrillated cellulose; cellulose nanocrystals; fullerenes; graphene; carbon nanotubes; diamond nanoparticles; sensors; drug delivery; tissue engineering; wound dressing

1. Introduction

Nanocellulose/nanocarbon composites are hybrid materials containing cellulose and carbon nanoparticles. Integration of nanocarbon materials with nanocellulose provides functionality of nanocarbons, using an eco-friendly, low-cost, strong, dimension-stable, nonmelting, nontoxic and nonmetal matrix or carrier, which alone has versatile applications in industry, biotechnology and biomedicine (for a review, see [1,2]). In addition to its advantageous combination with nanocarbon materials, nanocellulose is an appealing material for biomedical applications due to its tunable chemical

properties, nonanimal origin, and resemblance to biological molecules in dimension, chemistry and viscoelastic properties, etc. [3–6].

Cellulose nanomaterials include cellulose nanofibrils (CNFs) and cellulose nanocrystals (CNCs) [3]. CNFs are manufactured using either a bottom-up or a top-down approach. The bottom-up approach involves bacterial (*Gluconacetobacter*) biosynthesis to obtain bacterial cellulose (BC), while, in the top-down method, cellulosic biomass from plant fibers is disintegrated into smaller CNFs [7] that contain amorphous and crystalline regions [3]. The fibrillation of cellulose is achieved using mechanical forces, chemical treatments, enzymes or combinations of these. After fibrillation, the width of CNFs is typically between 3 and 100 nm, and the length can be several micrometers [8]. Separation of the crystalline parts from the amorphous regions of the fibers or fibrils to obtain CNCs typically requires acid hydrolysis, which destroys the amorphous regions [9]. Entangled CNFs are longer, while CNCs possess shorter needle- or rod-like morphology with a similar diameter and a more rigid molecule due to their higher crystallinity [3,9]. In general, the properties of nanocelluloses are variable and depend on their origin, type, processing, pretreatments and functionalization. Integration with other materials, as well as fabrication of the final product, further affects the properties of the resulting composite or hybrid structure.

Carbon nanoparticles include fullerenes (usually C_{60}), graphene-based particles (graphene, graphene oxide, reduced graphene oxide, graphene quantum dots), nanotubes (single-walled, double-walled, few-walled or multi-walled) and nanodiamonds (for a review, see [10–20]). The most frequently used nanocellulose/nanocarbon composites contain graphene or carbon nanotubes, while composites of nanocellulose with nanodiamond, and particularly with fullerenes, are less frequently used. Other carbon nanostructures, which are less frequently used in nanocellulose/nanocarbon composites, at least for biomedical applications, include carbon nanofibers [21–25], carbon quantum dots [26–28] activated carbon [29,30] and carbon black [31–33].

Nanocellulose/nanocarbon composites can be prepared in one-dimensional (1D), two-dimensional (2D) or three-dimensional (3D) forms. 1D composites are represented, for example, by C_{60} fullerenes grafted onto cellulose nanocrystals that have undergone amination or oxidation [34,35]. 2D composites are represented by films, which can be self-standing or supported, i.e., in the form of free-standing membranes [29,36–41] or in the form of coatings deposited on bulk materials [33,42]. The films can be formed by depositing carbon nanoparticles on a nanocellulose layer [43,44]. More frequently, however, they are fabricated from aqueous dispersions of nanocellulose and carbon nanoparticles [39,42]. It should be pointed out that cellulose nanoparticles are excellent dispersive agents for carbon nanoparticles, as they prevent the aggregation of these nanoparticles and maintain them in long-term stable homogeneous suspensions without the need to subject them to chemical functionalization [45,46]. Suspensions of cellulose and carbon nanoparticles are also starting materials for the creation of 3D nanocellulose/nanocarbon composites in the form of aerogels, foams or sponges [45,47–50]. In addition, composite 3D scaffolds, especially for tissue engineering and for regenerative medicine, can be fabricated by 3D printing using bioinks based on cellulose and carbon nanoparticles [51,52]. Both 2D composites and 3D composites can also be created by adding carbon nanoparticles to cultures of cellulose-producing bacteria, such as *Gluconacetobacter xylinus*. These nanoparticles are then incorporated into bacterial nanocellulose in situ during its growth [53–57]. Another approach is via the electrospinning or wet spinning of solutions containing cellulose and carbon nanoparticles [58–60].

Nanocellulose/nanocarbon composites exhibit several more advantageous properties than materials containing only cellulose nanoparticles or only carbon nanoparticles. Adding carbon nanoparticles to nanocellulose materials can further increase their mechanical strength [59,61]. At the same time, the presence of nanocellulose promotes the flexibility and stretchability of the materials [52,62,63]; for a review, see [64]. Adding graphene, carbon nanotubes or boron-doped diamond nanoparticles endows nanocellulose materials with electrical conductivity [39,50,57,65,66]. Other advantageous properties of nanocellulose/nanocarbon composites include their thermal stability [67–69], tunable thermal conductivity and optical transparency [48,57,70], intrinsic

fluorescence and luminescence [26,71,72] photothermal activity [56], hydrolytic stability [61], nanoporous character and high adsorption capacity [49,61]. Nanocellulose/nanocarbon composites can therefore be used in a wide range of industrial and technological applications, such as water purification [22,29,43,49,54,56,61,73–76], the isolation and separation of various molecules [22,74,77–79], energy generation, storage and conversion [21,23,44,47,64,80–85], biocatalysis [86], food packaging [67–69,87], construction of fire retardants [48], heat spreaders [70] and shape memory devices [38,88–90]. These composites are also used as fillers for various materials, usually polymers, in order to improve their mechanical, electrical and other physical and chemical properties [67–69,87,91].

In addition, nanocellulose/nanocarbon composites are promising for biomedical applications, though these applications are less frequent than industrial applications. Biomedical applications include radical scavenging [34,92], photothermal ablation of pathogenic bacteria [93], photodynamic and combined chemophotothermal therapy against cancer [35,94], drug delivery [16,28,65,72,95–97], biosensorics [31–33,63,66,71,91,98–104], and particularly tissue engineering and wound dressings. Hybrid materials containing nanocellulose and nanocarbons stimulated the growth and osteogenic differentiation of human bone marrow mesenchymal stem cells [37,59]. They provided good substrates for the attachment, growth and differentiation of SH-SHY5Y human neuroblastoma cells [51] and PC12 neural cells, particularly under electrical stimulation [105]. They enhanced the outgrowth of neurites from rat dorsal root ganglions in vitro and stimulated nerve regeneration in rats in vivo [106]. They also promoted the growth of vascular endothelial cells, enhanced angiogenesis and arteriogenesis in a chick chorioallantoic membrane model [107], and improved cardiac conduction when applied to surgically disrupted myocardium in dogs [52]. In addition, these materials supported the growth of human dermal fibroblasts [108] and mouse subcutaneous L929 fibroblasts [58,62], promoted wound healing in vivo in mice [109] and showed an antibacterial effect [30]. These materials are therefore promising for bone, neural and vascular tissue engineering, for creating cardiac patches and for advanced wound dressings. The biomedical applications of nanocellulose/nanocarbon composites are summarized in Table 1.

Table 1. Biomedical applications of nanocellulose/nanocarbon composites.

Application	Nanocellulose/Nanocarbon Composites Containing:				
	Fullerenes	**Graphene**	**CNTs**	**Nanodiamonds**	**Others**
Radical scavenging	NH_2-CNC/C_{60} [34]; CNC/$C_{60}(OH)_{30}$ [92]				
Photodynamic cancer therapy	TEMPO-oxidized CNC/C_{60}-NH_2 [35]				
Photothermal, chemo-photothermal therapy		Bacteria: [93]			
		Cancer: [94]			
Drug delivery		Anticancer drugs (doxorubicin) [72,95,96]	Anticancer and other drugs [16]	Anticancer drugs (doxorubicin) [97]	Carbon quantum dots: Anticancer drugs (temozolomide) [28]
(Bio)sensors		Electrochemical: cholesterol [98]; glucose and bacteria [110]; avian leucosis virus [111]; organic liquids [112]	Electrochemical: ATP metabolites [102]; oxygen [84]	Electrochemical: Biotin [66]	Carbon black: Electrochemical aptasensor for *S. aureus* [32]; electrochemical sensor for H_2O_2 [33]
		Piezoelectric: strain, human motion [63,99,113]	Piezoresistance and thermoelectric-based: pressure and temperature [103]; pressure [17]; strain, human motion [90,91,114]; humidity, human breath [104]		Carbon black: Strain, human motion [31,33]
	Optical: oxygen and temperature [115]; oxygen [116]	Optical: *SERS*: bilirubin [100]; *Fluorescence*: laccase [71]			Carbon quantum dots: optical sensor for biothiols [26]
		Acoustic: ammonia [101]			
Isolation of biomolecules		Histidine-rich proteins, hemoglobin [77]; bovine serum albumin [79]			
Electrical stimulation of tissues			Cardiac tissue [52]; neural tissue [106]		
Tissue engineering (TE)		General cell biocompatibility [68,69,87]; bone TE [37,59]; neural TE [105]; vascular TE [107]	Neural tissue engineering [51]; TE in general [117]		
Wound dressing/healing	Polysaccharides/fullerene C_{60} derivatives [118]	Human dermal fibroblasts in vitro [108]; mouse model in vivo [109]		L929 fibroblasts in vitro [58,62]; HeLa cells in vitro, wound dressings delivering doxorubicin [97]	Activated carbon: antibacterial wound dressing [30]

This review summarizes recent knowledge on the types, properties and applications of nanocellulose/nanocarbon-based hybrid materials, particularly in biotechnology, biomedicine and tissue engineering, and reports on the experience acquired by our group.

2. Nanocellulose/Fullerene Composites

2.1. Characterization of Fullerenes

Fullerenes are spheroidal cage-like molecules composed entirely of carbon atoms (Figure 1a). Fullerenes with 60 and 70 carbon atoms (C_{60} and C_{70}) are the most stable molecules, and they are therefore most frequently used in industrial and biomedical applications. Fullerenes were discovered in 1985 by Sir Harold Walter Kroto (1939–2016) and his co-workers Richard Smalley, Robert Curl, James Heath and Sean O'Brien. Kroto, Smalley and Curl were awarded the Nobel Prize in 1996. Fullerenes were named after Richard Buckminster "Bucky" Fuller (1895–1983), an American architect, designer, futurist, inventor, poet and visionary, who designed his geodesic dome on similar structural principles (for a review, see [12,13,18,119,120]). Fullerenes are carbon nanoparticles with diverse biological activities. This is due to the fact that they can act as either acceptors or donors of electrons (for a review, see [121]). The acceptor activity can lead to oxidative damage to cell components, such as DNA, cell membrane, mitochondria and various enzymes, to the activation of inflammatory reactions, and to cell apoptosis. These harmful effects of fullerenes can, however, be utilized for photodynamic therapy against tumors and pathogenic microorganisms (for a review, see [122]). The electron donor activity is associated with quenching oxygen radicals, which can be used in protecting skin against UV irradiation, in anti-inflammatory therapy against osteoarthritis, in cardioprotection during ischemia, in neuroprotection during amyloid-related diseases, damage by alcohol or heavy metals, in obesity treatment and in the treatment of diabetes-related disorders. Due to their structural analogy with clathrin-coated vesicles, fullerenes are also promising candidates for drug and gene delivery (for a review, see [12,13,18,119]).

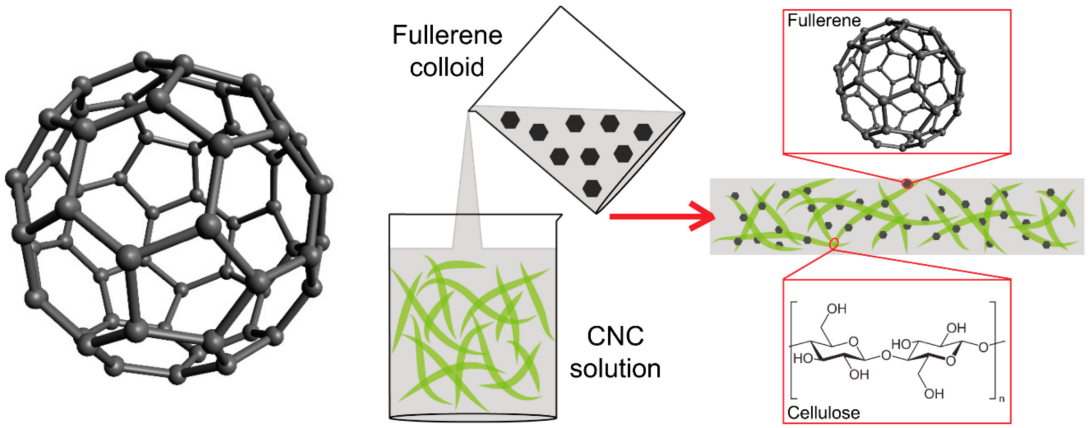

Figure 1. Scheme of fullerene C_{60} (**a**) and of the preparation and structure of nanocellulose/fullerene composites (**b**).

However, fullerenes have low solubility in many solvents, especially in water. This is a major drawback for their wider application in biomedical applications. The water solubility of fullerenes can be achieved by functionalizing them with hydrophilic groups, but this approach does not solve problems arising from the aggregation and clustering of fullerenes. In addition, the formation of singlet oxygen, which is needed for photodynamic therapy, decreases after functionalization due to the perturbation of the fullerene π system. These problems can be mitigated by the complexation of fullerenes with water-soluble agents, including nanocellulose [35].

2.2. Preparation and (Bio)Application of Nanocellulose/Fullerene Composites

Cellulose nanocrystals (CNCs) were used to create nanocellulose/fullerene composites. These nanocrystals are typically produced by acid hydrolysis of cellulose fibers, employing either sulfuric acid or hydrochloric acid in order to destroy the amorphous regions of the cellulose, while the crystalline segments remain intact. CNCs can have a needle-like or rod-like morphology, and are also referred to as nanowhiskers or nanorods. This morphology is characterized by a high aspect ratio (i.e., high length to diameter ratio), and thus by a relatively large surface area. In addition, CNCs have a wide range of other advantageous properties, such as high mechanical resistance, broad chemical-modifying capacity, renewability, biodegradability and low cytotoxicity [34,35]; for a review, see [2]. From these points of view, CNCs were considered ideal for immobilization of fullerene nanoparticles [92]. A scheme of preparation of nanocellulose/fullerene composites is depicted in Figure 1b. Composites of CNCs with fullerenes C_{60} were prepared by amine functionalization of CNCs and by subsequently grafting C_{60} onto the surface of amine-terminated CNCs [34]. Conversely, functionalized fullerenes, e.g., polyhydroxylated fullerenes $C_{60}(OH)_{30}$, were conjugated with the surface of CNCs [92]. Both of these composites showed a higher radical scavenging capacity in vitro than fullerenes alone, and therefore are promising for biomedical application in antioxidant therapies, e.g., as components of skin care products. In the third type of composites, both cellulose nanocrystals and fullerenes were functionalized, i.e., amino-fullerene C_{60} derivatives were covalently grafted onto the surface of 2, 2, 6, 6-tetramethylpiperidine-1-oxylradical (TEMPO)-oxidized nanocrystalline cellulose [35]. These composites hold promise for photodynamic cancer therapy (Table 1). When these composites were added to the culture medium of human breast cancer MCF-7 cells in the dark, they were taken up by these cells without changes in the cell viability, as revealed by a resazurin assay. However, when irradiated with light, these composites showed dose-dependent toxicity for MCF-7 cells [35].

However, fullerenes are less widely used in nanocellulose/nanocarbon composites than other carbon allotropes, particularly graphene and carbon nanotubes. More frequently, fullerenes are incorporated into a non-nanostructured cellulose matrix. For example, fullerene C_{70}, characterized by a strong thermally activated delayed fluorescence at elevated temperatures, which is extremely oxygen sensitive, was incorporated into ethyl cellulose, i.e., a highly oxygen-permeable polymer. This composite was used for construction of an optical dual sensor for oxygen and temperature [115]. An oxygen sensor was constructed using isotopically enriched carbon-13 fullerene C_{70}, dissolved in an ethyl cellulose matrix [116]. Mixed-matrix membranes, consisting of ethyl cellulose as a continuous matrix and fullerenes C_{60} as a dispersed phase, were prepared for propylene/propane separation [78]. Electrospun cellulose acetate nanofibers reinforced with fullerenes were used in the construction of dry-type actuators [123]. Cellulose impregnated with fullerenes C_{60} dissolved in o-xylene showed greater extraction efficiency for Cu^{2+}, Ni^{2+} and Cd^{2+} ions from an aqueous environment than the pure polymer [124]. Biocompatible composites containing polysaccharides (cellulose, chitosan and gamma-cyclodextrin) and fullerene derivatives (amino-C_{60} and hydroxy-C_{60}) were developed for various applications ranging from dressing and treating chronically infected wounds to nonlinear optics, biosensors, and therapeutic agents [118].

3. Nanocellulose/Graphene Composites

3.1. Characterization of Graphene

Graphene is a single layer of sp^2-hybridized carbon atoms arranged into a two-dimensional honeycomb-like lattice (Figure 2a). In other words, graphene is a one-atom-thick layer of graphite. It is a basic building block for other carbon allotropes, such as fullerenes, carbon nanotubes and graphite. Graphene is a very thin, nearly transparent sheet, but it is remarkably strong (about 100 times stronger than steel), and highly electrically and thermally conductive (for a review, see [19,20,125,126]). Graphene can be prepared by various methods, which can be divided into two main categories, namely the top-down approach and the bottom-up approach. The top-down approaches include treatment of

graphite by mechanical or electrochemical exfoliation, intercalation or sonication, and also nanotube slicing. The bottom-up approaches include growth of graphene from carbon-metal melts, epitaxial growth of graphene on silicon carbide, the dry ice method, and deposition methods such as chemical vapor deposition or dip coating a substrate with graphene oxide (GO), followed by GO reduction (for a review, see [19,20,125,126]). Graphene can be prepared in the form of monolayer or bilayer sheets, nanoplatelets, nanoflakes, nanoribbons and nanoscrolls. Chemically, graphene-based materials include pure graphene sheets, GO or reduced graphene oxide (rGO). Pure graphene sheets can be produced by mechanical exfoliation of graphite or by chemical vapor deposition. GO, a highly oxidative and water-soluble form of graphene, can be obtained by the exfoliation of graphite oxide. Reduced GO can be prepared by chemical, thermal or pressure reduction, and even by bacteria-mediated reduction of GO, which improves its electrical properties (for a review, see [13,18,19,37,125,126]). Graphene and graphene-based materials hold a great promise not only for a wide range of industrial and technology applications, but also for biomedical applications, such as drug, gene and protein delivery, photothermal therapy, construction of biosensors, bioimaging, antimicrobial treatment, and also as scaffolds for tissue engineering (for a review, see [20]).

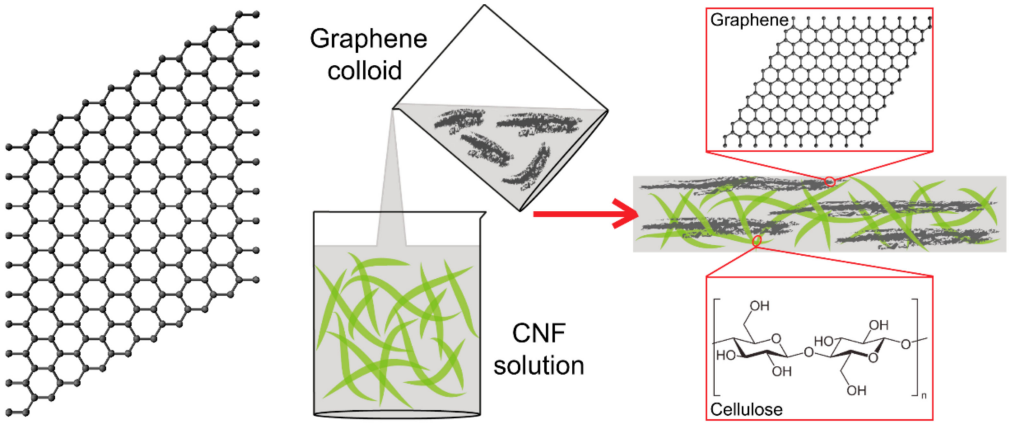

Figure 2. Scheme of graphene (**a**) and of the preparation and structure of nanocellulose/graphene composites (**b**).

3.2. Preparation and Industrial Application of Nanocellulose/Graphene Composites

Similarly as in fullerenes, cellulose nanoparticles in the form of nanofibrils and nanocrystals increase the dispersion of graphene nanoparticles in water-based environments and prevent their aggregation without the need to subject them to chemical functionalization [46]. A water-based dispersion is the starting material for fabricating nanocellulose/graphene composites (Figure 2b). These composites can be created by filtration [127], filtration combined with hot pressing for fabricating films [128], or by freeze-drying [75] and freeze-casting [48] for fabricating 3D materials, such as aerogels and foams. Other methods are deposition of graphene on a nanocellulose layer [43] and incorporation of graphene into nanocellulose during its biological synthesis by bacteria [54–56].

All forms of nanocellulose and graphene have been used for constructing nanocellulose/graphene composites, i.e., CNFs, CNCs, unmodified graphene, GO and rGO. In order to modulate the properties of nanocellulose/graphene composites for specific applications, these materials can be further enriched by various substances, such as metallic or ceramic nanoparticles, oxides, carbides, sulfides, vitamin C, synthetic and natural polymers, enzymes and antibodies. For example, nanocellulose/graphene composites have high adsorption, filtration and photocatalytic ability, and they are therefore widely used for water purification, e.g., for removing antibiotics [75], dyes [43], heavy metals, such as Cu^{2+}, Hg^{2+}, Ni^{2+} and Ag^{+} [61,76], or for their bactericidal effect [56]. The water-cleaning capacity of these composites can be further enhanced by introducing additional photocatalytic agents, i.e., palladium

nanoparticles [54] or zinc oxide (ZnO) nanoparticles [73]. An optimized ultrafiltration membrane for water purification was constructed from polyvinylidene fluoride (PVDF), modified by cellulose nanocrystals functionalized with common bactericides, such as dodecyl dimethyl benzyl ammonium chloride, ZnO and GO nanosheets [129]. Another important additive is vitamin C, which reduces the GO in nanocellulose/GO composites, increases the surface area of the material and increases pore formation, and thus enhances the capacity of the composites for water purification [49]. A combination of rGO-coated cellulose nanofibers with hydrophobic and oleophilic trimethyl chlorosilane enhanced the adsorption capacity of this composite, which is necessary for effective removal of oil-based pollutants from water [74].

Another important industrial application of nanocellulose/graphene composites is in energy storage, generation and conversion. Devices for these purposes include supercapacitors [64,80,130], hydrogen storage devices [131], electrodes for hydrogen evolution reaction [132], lithium ion batteries [133], actuators [81], solar steam generators [82] and electric heating membranes [83]. These devices can be based on pure nanocellulose/nanocarbon composites without additives [80–83]. However, they often contain additives such as manganese oxide (MnO), which contributes to faradaic pseudocapacitance in supercapacitors [130] or polypyrrole, which acts as an insulator, but its oxidized derivatives are good electrical conductors [134]. Other additives are palladium or platinum nanoparticles for enhanced hydrogen storage [131], nitrogen-doped molybdenum carbide nanobelts in electrocatalysts for hydrogen evolution reaction [132], and silicon oxide nanoparticles in lithium ion batteries [133].

Other important industrial applications of nanocellulose/graphene composites are in the construction of fire retardants, shape memory devices, biocatalysts and materials for food packaging. Super-insulating, fire-retardant, mechanically strong anisotropic foams were produced by freeze-casting suspensions of cellulose nanofibers, GO and sepiolite nanorods, and they performed better than traditional polymer-based insulating materials [48]. Shape memory devices are based on GO/CNC thin films and nanomembranes [38,88] or on GO introduced into a nanocellulose paper made of nanofibers extracted from sisal fibers [89]. An example of a biocatalyst is a nanocellulose/polypyrrole/GO nanocomposite for immobilization of lipase, a versatile hydrolytic enzyme. This biocatalyst was employed for synthesizing ethyl acetoacetate, a fruit flavor compound [86]. Food packaging materials were constructed by filling CNCs and rGO, either separately or in the form of CNC/rGO nanohybrids, into poly (lactic acid) (PLA) matrix or in a poly (3-hydroxybutyrate-*co*-3-hydroxyvalerate) (PHBV) matrix. These composite materials exhibited better mechanical properties than the pristine polymers, and possessed antibacterial activity. In addition, the composites with CNC/rGO nanohybrids performed better than those with a single component nanofiller, i.e., either CNCs or rGO. Due to their antibacterial activity, antioxidant properties and good in vitro cytocompatibility, these composites are also promising for biomedical applications, e.g., as scaffolds for tissue engineering [67–69,87].

3.3. Biomedical Application of Nanocellulose/Graphene Composites

The biomedical applications of nanocellulose/nanographene composites include photothermal ablation of pathogenic bacteria, combined chemo-photothermal therapy against cancer, drug delivery, biosensorics, isolation and separation of various biomolecules, wound dressing and particularly tissue engineering (Table 1).

For photothermal ablation of pathogenic bacteria, a composite paper containing nanocellulose with Au linked to GO using quaternized carboxymethyl chitosan was developed. When excited by near-infrared laser irradiation, the paper generated a rise in temperature of more than 80 °C, sufficient for photothermal ablation, both on Gram-positive bacteria (*Bacillus subtilis* and *Staphylococcus aureus*) and on Gram-negative bacteria (*Escherichia coli* and *Pseudomonas aeruginosa*). Additionally, the composite paper showed a remarkable enhancement in tensile strength, bursting index and tear index in comparison with the properties of pure nanocellulose paper [93].

For chemophotothermal synergistic therapy of colon cancer cells, dual stimuli-responsive polyelectrolyte nanoparticles were developed by layer-by-layer (LbL) assembly of aminated nanodextran and carboxylated nanocellulose on the surface of chemically modified GO. Tests on the HCT116 human colon cancer cell line revealed that these nanoparticles allowed for the intracellular delivery of curcumin, which was released in response either to acidic environments or to near-infrared excitation [94]. In this context, nanocellulose/graphene composites are good candidates as carriers for controlled drug delivery, particularly of anticancer drugs. Systems releasing doxorubicin, a model drug with broad-spectrum anticancer properties, were developed. These systems included nanocomposite carboxymethyl cellulose/GO hydrogel beads [95], nanocomposite films made of graphene quantum dots incorporated into a carboxymethyl cellulose hydrogel [72] or macroporous polyacrylamide hydrogels. These hydrogels were prepared using an oil-in-water Pickering emulsion, containing GO and hydroxyethyl cellulose with a quaternary ammonium group [96].

Sensing and biosensing is another important application of nanocellulose/graphene composites. These sensors can be divided into electrochemical, piezoelectric, optical and acoustic wave-based sensors. Electrochemical sensors were constructed for detecting cholesterol [98], glucose and pathogenic bacteria [110], avian leucosis virus [111] and organic liquids [112]. The biosensor for detecting cholesterol was based on chemically-modified nanocellulose, grafted with silylated GO and enriched with ZnO nanoparticles in order to enhance its electrical conductivity [98]. The biosensor for detecting glucose and pathogenic bacteria was based on nanocellulose paper coated with GO, reduced by vitamin C and functionalized with platinum nanoparticles with a cauliflower-like morphology in order to enhance the electrical conductivity of the composite. The platinum surface was functionalized either with glucose oxidase (via chitosan encapsulation) or with an RNA aptamer [110]. The biosensor for the avian leucosis virus was an immunosensor, based on graphene-perylene-3, 4, 9, 10-tetracarboxylic acid nanocomposites as carriers for primary antibodies, on composites of nanocellulose and Au nanoparticles as carriers for secondary antibodies, and on the alkaline phosphatase catalytic reaction [111]. The sensor for organic liquids, mainly organic solvents, was based on cellulose nanocrystal-graphene nanohybrids, selectively located in the interstitial space between the natural rubber latex microspheres [112].

Piezoelectric nanocellulose/graphene-based sensors have usually been designed for strain sensing, i.e., as wearable electronics for monitoring the motion of various parts of the human body, e.g., fingers [63,99,113]. For these purposes, the flexibility and stretchability of nanocellulose was further enhanced by adding other polymers, such as elastomers, represented e.g., by polydimethylsiloxane (PDMS) [113], or hydrogels, represented e.g., by poly(vinyl alcohol) (PVA), crosslinked (together with cellulose nanofibers and graphene) with borax [63].

Optical sensors can be based on surface-enhanced Raman spectroscopy (SERS) or fluorescence. Cellulose SERS strips decorated with plasmonic nanoparticles, termed graphene-isolated-Au-nanocrystals (GIANs), were developed for constructing portable sensors for detecting complex biological samples, e.g., for detecting free bilirubin in the blood of newborns [100]. A fluorescence sensor, based on sulfur and nitrogen-co-doped graphene quantum dots, immersed into nanocellulosic hydrogels, was developed for detecting laccase. This enzyme is widely used in industrial and technological applications, such as bleaching of fabrics, tooth whitening, decoloration of hair, water purification and in oxidizing dyes in beer, must and wines [71].

An example of an acoustic wave-based sensor is an ammonia sensor, based on a quartz crystal microbalance (QCM) with a sensing coating. This coating is composed of negatively-charged electrospun cellulose acetate nanofibers, positively-charged polyethylenimine and negatively-charged GO, and it was created by the electrostatic LbL self-assembly technique [101].

For protein isolation, a metal affinity carboxymethyl cellulose-functionalized magnetic graphene was prepared by successive modifications of GO nanosheets with magnetic nanoparticles, carboxymethyl cellulose and iminodiacetic acid, and then chelated with copper ions. This composite exhibited high adsorption selectivity toward histidine-rich proteins, which was utilized for isolating hemoglobin from human whole blood, and also for isolating a polyhistidine-tagged recombinant

protein from *Escherichia coli lysate*, namely *Staphylococcus aureus* enterotoxin B [77]. For macromolecular separation, cellulose acetate nanocomposite ultrafiltration membranes were fabricated using 2D layered nanosheets, e.g., GO and exfoliated molybdenum disulfide (MoS_2), and were successfully tested using macromolecular bovine serum albumin [79].

Nanocellulose/graphene composites are also important components of tissue engineering scaffolds, improving their mechanical properties and their bioactivity. In the studies by Pal et al. (2017), mentioned above, a PLA/CNC/rGO nanocomposite film showed antibacterial activity against Gram-positive *Staphylococcus aureus* and against Gram-negative *Escherichia coli*. At the same time, this film exhibited negligible cytotoxicity against a mouse NIH-3T3 fibroblast cell line, as revealed by an MTT assay of the activity of mitochondrial oxidoreductase enzymes [87]. Nanocomposites of CNCs and rGO, incorporated into PLA matrix through the melt-mixing method, were noncytotoxic and cytocompatible with epithelial human embryonic kidney 293 (HEK293) cells [68]. PLA incorporated with rGO and TEMPO-oxidized CNCs, grafted with poly(ethylene glycol) (PEG), displayed radical scavenging activity and negligible toxicity and cytocompatibility to mouse embryonic C3H10T1/2 cells [69]. A composite film consisting of hydrophilic bacterial cellulose nanofibers and hydrophobic rGO, prepared from GO using a bacterial reduction method, supported the adhesion, viability and proliferation of human bone marrow mesenchymal stem cells in a similar way to standard cell culture polystyrene, and better than pure rGO films [37]. Incorporating GO into electrospun cellulose acetate nanofibrous scaffolds enhanced the adhesion and growth of human umbilical cord mesenchymal stem cells. It also enhanced osteogenic differentiation of these cells, manifested by the activity of alkaline phosphatase, and biomineralization of the scaffolds in a simulated body fluid [59]. Nanofibrous composites of bacterial nanocellulose, a conductive poly(3,4-ethylene dioxythiophene) (PEDOT) polymer and GO, mimicking the native extracellular matrix and allowing electrical stimulation of neural PC12 cells, induced specific orientation and differentiation of these cells [105]. Polyvinyl alcohol/carboxymethyl cellulose (PVA/CMC) scaffolds loaded with rGO nanoparticles, prepared by lyophilization, enhanced the proliferation of EA.hy926 endothelial cells in vitro and angiogenesis in vivo using a chick chorioallantoic membrane model [107]. Polyacrylamide-sodium carboxymethylcellulose hybrid hydrogels reinforced with GO and/or CNCs also have potential for tissue engineering applications due to their tunable mechanical properties [135]. Genetically modified hydrophobin, a fungal cysteine-rich protein, was used to connect nanofibrillated cellulose of wood origin and graphene flakes in order to construct biomimetic mechanically-resistant materials similar to nacre and combining high toughness, strength and stiffness [136].

Nanocellulose/graphene composites also have great potential for the fabrication of antibacterial textiles and for advanced wound dressing. Antibacterial textiles were prepared by electrospinning a mixture containing cellulose acetate, TiO_2 and GO sheets. These textiles showed high antibacterial activity with an inhibition rate higher than 95% against *Bacillus subtilis* and *Bacillus cereus* [137]. Bacterial cellulose is considered as one of the most suitable materials for advanced wound dressing, due to its appropriate mechanical properties, such as strength, Young's modulus, elasticity and conformability, and also due to its great capacity to retain moisture in the wound (for a review, see [2]). These favorable properties can be further enhanced by adding graphene-based materials and by crosslinking with synthetic polymers, such as poly (ethylene glycol), poly (vinyl alcohol), poly (acrylic acid) and poly (acrylamide). In a study by Chen et al. (2019), a bacterial nanocellulose-grafted poly (acrylic acid)/GO composite hydrogel was prepared as a potential wound dressing. The inclusion of GO improved the attachment and proliferation of human dermal fibroblasts in cultures on the composites [108]. Similarly, hydroxypropyl cellulose matrix incorporated with GO and silver-coated ZnO nanoparticles showed improved tensile strength, and also anti-ultraviolet, antibacterial and immunostimulatory effects, which promoted wound healing in an in vivo mouse model [109].

4. Nanocellulose/Carbon Nanotube Composites

4.1. Characterization of Carbon Nanotubes

Carbon nanotubes (CNTs; Figure 3a) are tubular structures formed by a single cylindrical graphene sheet (single-walled carbon nanotubes, referred to as SWCNTs or SWNTs) or several graphene sheets arranged concentrically (multiwalled carbon nanotubes, referred to as MWCNTs or MWNTs, which also include double-walled CNTs (DWCNTs [16]), and few-walled CNTs (FWCNTs [17]). Carbon nanotubes were discovered as a by-product of fullerene synthesis, and were first described by Iijima et al. (1991) [138]. CNTs have a high aspect ratio (i.e., length to diameter ratio) and thus a relatively large surface area. Their diameter is on the nanometer scale (e.g., from 0.4 nm to 2–3 nm in single-walled nanotubes), but their length can reach several micrometers or even centimeters. Due to these properties, CNTs are suitable candidates for hydrogen storage, for the removal of contaminants from water and air, and also for drug delivery. CNTs have excellent mechanical properties, mainly due to the sp^2 bonds. The tensile strength of SWCNTs has been reported to be almost 100 times higher than that of steel, while their specific weight is about six times lower. CNTs can therefore be used for reinforcing various synthetic and natural polymers for industrial and biomedical applications, e.g., for hard tissue engineering. When added to a polymer matrix, CNTs can resemble inorganic mineral nanoparticles in the bone tissue, and they can form nanoscale irregularities on the surface of 2D materials and in the pores of 3D materials, which improve the cell adhesion and growth. CNTs are electrically conductive and enable electrical stimulation of cells, which further improves the adhesion, growth and differentiation of cells (for a review, see [10–14,18,139]). However, free CNTs can be cytotoxic, which is attributed to their ability to cause oxidative damage, and also to their contamination with transition metals (e.g., Fe, Ni, Y), which serve as catalysts during CNT preparation. Methods for producing metal-free CNTs have therefore been developed, e.g., arc-discharge evaporation of graphite rods [139].

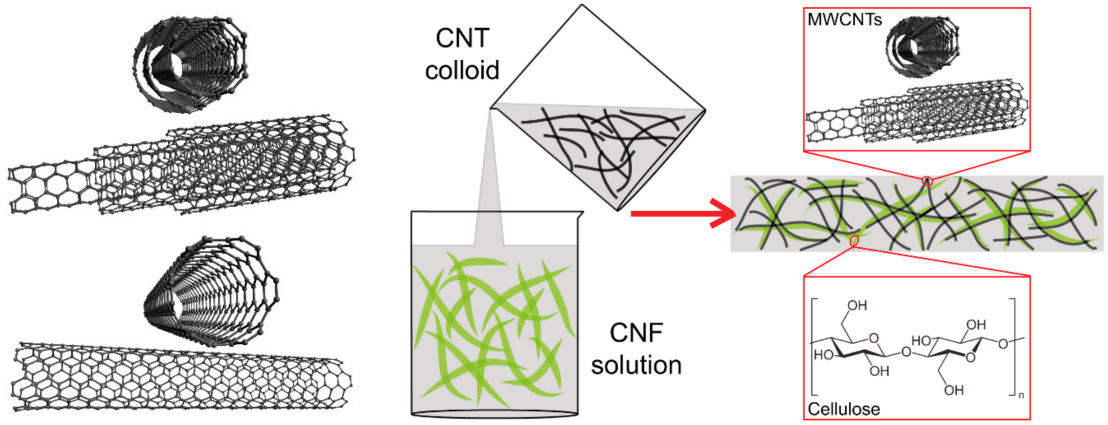

Figure 3. Scheme of multi-walled and single-walled carbon nanotubes (**a**) and of the preparation and structure of nanocellulose/carbon nanotube composites (**b**).

CNTs also resemble CNFs from the point of view of their morphology and their mechanical properties. For example, highly crystalline, thick CNFs derived from tunicates exhibited mean strength of 3–6 GPa, which was comparable with commercially available MWCNTs. However, the mean strength of other types of CNFs is lower; for example, in wood-derived CNFs the mean strength ranged from 1.6 to 3 GPa [140]. CNTs therefore improve the mechanical strength of nanocellulose/CNT composites, and endow them with electrical conductivity, similarly as graphene. As a result, nanocellulose/CNT composites are used in similar industrial and biomedical applications as nanocellulose/graphene composites, e.g., water purification, energy generation, storage and conversion, filling polymeric materials, constructing sensors and biosensors, drug delivery, cancer treatment, electrical stimulation of tissues, and tissue engineering.

4.2. Preparation and Industrial Application of Nanocellulose/CNT Composites

The nanocellulose component in the nanocellulose/CNT composites is used in the form of nanofibrils and nanocrystals, and carbon nanotubes usually in the form of SWCNTs or MWCNTs. Similarly as in composites containing graphene and other carbon allotropes, cellulose nanoparticles facilitate the homogeneous dispersion of CNTs in aqueous environments (Figure 3b), where the two types of nanoparticles are linked by noncovalent interactions, e.g., hydrophobic and electrostatic interactions [42,46]. The dispersion of CNTs can be further facilitated by TEMPO-mediated oxidation of cellulose nanoparticles, which endows them with abundant anionic carboxyl groups [141]. Other ways include the functionalization of CNTs with self-assembling amphiphilic glycosylated proteins [142] or the use of oil-in-water Pickering emulsions of cellulose nanoparticles [143]. From the aqueous dispersions, 2D and 3D nanocellulose/CNT composites can be formed, e.g., by vacuum filtration, centrifugal cast molding, foam forming, casting and printing [39,45,50,141]. Pickering emulsions of cellulose nanocrystals and SWCNTs or MWCNTs were used for fabricating aerogels and foams by freeze-drying [143]. Similarly as in nanocellulose/graphene composites, CNTs can be added to cultures of bacteria producing nanocellulose, and incorporated into the bacterial nanocellulose during its growth [53,57]. Composite nanocellulose/SWCNT films can be transparent or semitransparent [39,45,141], and can transmit radiant energy [144].

Like nanocellulose/graphene composites, nanocellulose/CNT composites can be combined with various atoms, molecules and nanoparticles in order to enhance their properties for specific applications. For example, Ag nanoparticles attached to the surface of MWCNTs influenced the electrochemical properties of CNT-based films developed on a bacterial nanocellulose membrane [36]. Nanocellulose and CNTs can be also used as additives to various hybrid materials. For example, a hybrid material, created by combination of poly (3,4-ethylenedioxythiophene)-poly (styrenesulfonate) (PEDOT:PSS), silver nanoparticles (AgNPs), CNTs and a nanocellulose layer, was used for constructing a tactile sensor [103]. Incorporation of polypyrrole-coated CNTs into chemically cross-linked CNC aerogels created promising materials for flexible 3D supercapacitors [145]. A combination of cellulose acetate, chitosan and SWCNTs with Fe_3O_4 and TiO_2 in electrospun nanofibers enables combined removal of Cr^{6+}, As^{5+}, methylene blue and Congo red from aqueous solutions via the adsorption and photocatalytic reduction processes [146].

Energy-related applications of nanocellulose/CNT composites include biofuel cells, varactors, supercapacitors, and electrodes for lithium batteries, thermoelectric generators for heat-to-electricity conversion or for constructing heating elements [50]. A biofuel cell comprising electrodes based on supercapacitive materials, i.e., on CNTs and a nanocellulose/polypyrrole composite, was utilized to power an oxygen biosensor. Laccase, immobilized on naphthylated MWCNTs, and fructose dehydrogenase, adsorbed on a porous polypyrrole matrix, were used as cathode and anode bioelectrocatalysts, respectively [84]. Another biofuel cell was based on a conductive MWCNT network, developed on a bacterial nanocellulose film, and functionalized with redox enzymes, including pyroquinoline quinone glucose dehydrogenase (anodic catalyst) and bilirubin oxidase (cathodic catalyst). This system generated electrical power via the oxidation of glucose and the reduction of molecular oxygen [44]. Microelectromechanical system varactors, i.e., voltage-controlled capacitors, consisted of a freestanding SWCNT film, which was employed as a movable component, and a flexible nanocellulose aerogel filling [85]. Supercapacitors with high physical flexibility, desirable electrochemical properties and excellent mechanical integrity were realized by rationally exploiting the unique properties of bacterial nanocellulose, CNTs, and ionic liquid-based polymer gel electrolytes [147]. Other flexible 3D supercapacitor devices were fabricated by incorporating polypyrrole nanofibers, polypyrrole-coated CNTs, and manganese dioxide (MnO_2) nanoparticles in chemically cross-linked cellulose nanocrystal aerogels [145]. Electrospun core-shell nanofibrous membranes, containing CNTs stabilized with cellulose nanocrystals, were developed for use as high-performance flexible supercapacitor electrodes with enhanced water resistance, thermal stability and mechanical toughness [40]. Electrodes for lithium batteries were based on freestanding

$LiCoO_2$/MWCNT/cellulose nanofibril composites, fabricated by a vacuum filtration technique [148], or on freestanding CNT-nanocrystalline cellulose composite films [41]. Thermoelectric generators for heat-to-electricity conversion were based on large-area bacterial nanocellulose films with an embedded/dispersed CNT percolation network, incorporated into the films during nanocellulose production by bacteria in culture [57]. Electrical energy can also be converted into thermal energy, as demonstrated by the composite structure of wood-derived nanocellulose, MWCNTs and pulp, designed for a heating element application [50].

4.3. Biomedical Application of Nanocellulose/CNT Composites

Biomedical applications of composites of cellulose and CNTs are summarized in Table 1. These composites are important systems for drug delivery. The CNTs in the composites can be conjugated with many therapeutics, usually anticancer drugs, but also other types of drugs. For example, an osmotic pump tablet system coated with cellulose acetate membrane containing MWCNTs was developed for delivery of indomethacin (for a review, see [16,65]). Cancer cells can be killed by nanocellulose-CNT dispersions even without the presence of anticancer drugs. For example, nonmercerized type-II cellulose nanocrystals in dispersions with SWCNTs displayed cytotoxicity for human epithelial colorectal adenocarcinoma Caco-2 cells, but they enhanced the mitochondrial metabolism of normal cells [149].

Construction of sensors and biosensors is another important application of nanocellulose/CNT composites useful for (bio) technology and medicine. A tactile piezoresistance and thermoelectric-based sensor, mentioned above, which is capable of simultaneously sensing temperature and pressure, is fabricated from TEMPO-oxidized cellulose, PEDOT:PSS, AgNPs and CNTs [103]. Another pressure sensor was developed using aerogels consisting of plant cellulose nanofibers and functionalized few-walled CNTs [17]. Highly conductive and flexible membranes with a semi-interpenetrating network structure, fabricated from MWCNTs and cellulose nanofibers, showed the electrical features of capacitive pressure sensors and were promising for various electronics applications, e.g., touch screens [150]. Advanced flexible strain sensors for controlling the human body motion were fabricated by pumping hybrid fillers consisting of CNTs/CNCs into porous electrospun thermoplastic polyurethane membranes [91]. Other strain sensors were fabricated by a facile latex assembly approach, in which CNCs played a key role in tailoring the percolating network of conductive natural rubber/CNT composites [114]. A water-responsive shape memory hybrid polymer, based on a thermoplastic polyurethane matrix crosslinked with hydroxyethyl cotton cellulose nanofibers and MWCNTs, was also developed for constructing a strain sensor [90]. A flexible and highly sensitive humidity sensor, capable of monitoring human breath, was based on TEMPO-oxidized nanofibrillated cellulose and CNTs [104]. An electrochemical biosensor for three adenosine triphosphate (ATP) metabolites, namely uric acid, xanthine and hypoxanthine, was based on a composite of NH_2-MWCNT/black phosphorene/AgNPs, dispersed in carboxymethyl cellulose [102]. Another electrochemical molecularly-imprinted sensor was based on a nanofibrous membrane prepared by the electrospinning technique from cellulose acetate, MWCNTs and polyvinylpyrrolidone, and was used for determining ascorbic acid [151]. An oxygen biosensor powered by a biofuel cell containing MWNCTs, a nanocellulose/polypyrrole composite, laccase and fructose dehydrogenase, was mentioned above [84]. Versatile wearable textile sensors, e.g., for gas sensing, were produced from cellulose nanofibers extracted from tunicates, homogeneously composited with SWCNTs, by wet spinning in an aligned direction [60].

Other important biomedical applications of nanocellulose/CNT composites are in electrical stimulation of cells and tissues in order to improve their regeneration and function, and in tissue engineering. For example, stretchable, flexible and electrically conductive biopatches for restorating conduction in damaged cardiac regions and for preventing arrhythmias were prepared. These patches were based on nanofibrillated cellulose/SWCNT ink three-dimensionally printed onto bacterial nanocellulose. They restored cardiac conduction after its disruption by a surgical incision made in the ventricular part of the heart in experimental dogs [52]. For neural tissue stimulation, multiblock

conductive nerve scaffolds with self-powered electrical stimulation were prepared. These scaffolds were based on polypyrrole/bacterial nanocellulose composites with platinum nanoparticles on the anode side for glucose oxidation, and nitrogen-doped CNTs on the cathode side for oxygen reduction. These scaffolds enhanced the elongation of neurites outgrowing from rat dorsal root ganglions in vitro and stimulated nerve regeneration in a rat sciatic nerve gap model in vivo in comparison with composites containing only polypyrrole and bacterial nanocellulose. These scaffolds could replace the metal needles that are currently used for external electrical stimulation of neural tissue, which may cause pain and a risk of infection [106]. 3D printing was also used for creating scaffolds based on a conductive ink composed of wood-derived CNFs and SWCNTs. These scaffolds were intended for neural tissue engineering for experimental brain studies, and supported the attachment, growth and viability of human neuroblastoma SH-SHY5Y cells [51]. Other scaffolds for tissue engineering consisted of electrospun cellulose acetate nanofibers, assembled with positively-charged chitosan and negatively-charged MWCNTs via an LbL technique. These scaffolds promoted the adsorption of cell adhesion-mediating molecules from the serum supplement of the culture medium and the adhesion and growth of mouse subcutaneous L929 fibroblasts [117]. Our own results related to the potential application of nanocellulose/CNT composites as scaffolds for tissue engineering are reported in Appendix A.

5. Nanocellulose/Nanodiamond Composites

5.1. Characterization of Nanodiamond

Diamond is an allotrope of carbon, consisting of carbon atoms arranged in a cubic crystal structure covalently bonded in sp^3 hybridization (Figure 4a). Like all nanostructured materials, nanodiamonds or diamond nanoparticles are defined as features not exceeding 100 nm in at least one dimension, although some larger diamond particles, i.e., 125–210 nm, are still referred to as nanodiamonds (for a review, see [152]). At the same time, the size of ultrananocrystalline diamond particles is 3–5 nm [153,154]. Diamond nanoparticles can be prepared by various methods. The most widely used techniques are detonation of carbon-containing explosives in an oxygen-deficit environment and microwave-enhanced plasma chemical vapor deposition (MECVD). Other techniques include the radiofrequency plasma-assisted chemical vapor deposition (PACVD) method, milling of diamond microcrystals, hydrothermal synthesis, ion bombardment, laser bombardment, ultrasound synthesis and electrochemical synthesis (for a review, see [10,152–156]). Nanodiamonds are considered to be the most advanced carbon materials in the world. This is due to their excellent mechanical, optical, electrical, thermal and chemical properties. The mechanical properties of nanodiamonds include the highest hardness of all materials on earth, a high Young's modulus, high fracture toughness, high pressure resistance and a low friction coefficient. Their optical properties include transparency, high optical dispersion, and their ability to display various colors and to emit intrinsic luminescence (fluorescence), which is due to defects in the diamond lattice or contamination of the lattice with foreign atoms, such as N, B, H, Ni, Co, Cr or Si. Regarding their electrical properties, nanodiamonds can act as good insulators in their pristine state and as semiconductors after doping, usually with boron. Their thermal properties include superior thermal conductivity and low thermal expansion. The chemical properties of nanodiamonds include low chemical reactivity and resistance to liquid- and gas-phase oxidations. However, nanodiamonds can be doped with various atoms, and their surface can be functionalized by various atoms, chemical groups and (bio)molecules ([152,153,157,158]; for a review, see [10–15,155]).

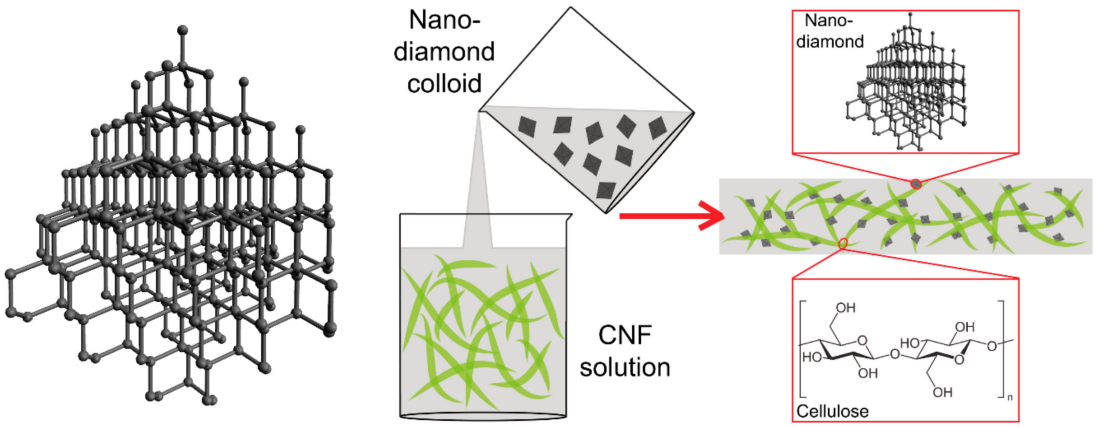

Figure 4. Scheme of a nanodiamond (**a**) and of the preparation and structure of nanocellulose/nanodiamond composites (**b**).

5.2. Preparation and (Bio)Application of Nanocellulose/Nanodiamond Composites

There is greater use of diamond nanoparticles than of fullerenes in nanocellulose/nanocarbon composites, but diamond nanoparticles are used less than graphene and carbon nanotubes. This may be because a nanodiamond is more expensive and is electrically nonconductive in its pristine state. In composites with nanofibrillated cellulose (Figure 4b), a nanodiamond was used for constructing highly thermally conductive, mechanically resistant and optically transparent films with potential application as lateral heat spreaders for portable electronic equipment [70]. A highly mechanically resistant and optically transparent nanopaper was made of cationic CNFs and anionic nanodiamond particles by filtration from a hydrocolloid and subsequent drying [159]. Moreover, a diamond can be rendered electrically semiconductive by doping it with boron, and then can be used for constructing biosensors. For example, a sensor for biotin was developed by the adsorption of captavidin, a nitrated avidin with moderate affinity to biotin, on a carboxymethylcellulose layer stabilized on a boron-doped diamond electrode by a Nafion film. This biosensor was used for analyzing biotin in blood plasma [66] (Table 1).

The reinforcing effect of diamond nanoparticles, coupled with their optical transparency, has also been used advantageously for other biomedical applications, particularly for wound dressing. Nanocellulose/nanodiamond composites are more mechanically resistant than purely nanocellulose-based materials, but they retain their flexibility and stretchability. In addition, their optical transparency enables direct inspection of wounds without the need to remove the dressing. For example, incorporating diamond nanoparticles in a concentration of 2 wt % into chitosan/bacterial nanocellulose composite films resulted in a 3.5-fold increase in the elastic modulus of these films. These composite films were transparent, but their transparency can be modulated by the concentration of diamond nanoparticles, turning them gray and semitransparent at higher nanodiamond concentrations (3 and 4 wt %). The viability of mouse subcutaneous L929 fibroblasts in cultures on these films, evaluated by an MTT test of the activity of cell mitochondrial enzymes, was more than 90% at 24 h after seeding. However, at 48 h, it had dropped to about 75%, which indicated that diamond nanoparticles are slightly cytotoxic [62]. A similar result was obtained on L929 fibroblasts grown on electrospun composite nanofibrous mats containing chitosan, bacterial cellulose and 1–3 wt % medical-grade nanodiamonds [58]. The viability of these cells, estimated by the MTT assay, dropped from approx. 90% on day 1 to approx. 75% on day 3. Nevertheless, the addition of nanodiamonds facilitated the electrospinning process, reduced the diameter of the nanofibers in the mats, regulated the water vapor permeability of the mats, enhanced their hydrophilicity and improved their mechanical properties to a similar level as in native skin [58].

Adding diamond nanoparticles per se did not significantly increase the antibacterial activity of chitosan/bacterial nanocellulose composites [62]. This activity can be further enhanced, e.g., by

adding silver nanoparticles [160]. Nanocellulose/nanodiamond composites can also act as a suitable platform for drug delivery. This was demonstrated on transparent doxorubicin-loaded carboxylated nanodiamonds/cellulose nanocomposite membranes, which are promising candidates for wound dressings. These membranes are porous, transparent, with appropriate mechanical properties, and without doxorubicin they are noncytotoxic for HeLa cells [97].

6. Composites of Nanocellulose with Other Carbon Nanoparticles

In addition to fullerenes, graphene, nanotubes and nanodiamonds, other important carbon nanoparticles used in industrial, biotechnological and biomedical applications include carbon nanofibers, carbon quantum dots and nanostructures formed by activated carbon and carbon black. All these nanomaterials can be used in nanocellulose/nanocarbon composites. The biomedical applications of these composites are summarized in Table 1.

6.1. Composites of Nanocellulose and Carbon Nanofibers

Carbon nanofibers can be created by carbonization of cellulose nanofibers originating from bacterial nanocellulose [21,23,161], urea [161], filter paper [162] or plant-derived cellulose [22,24]. Another method of preparing carbon nanofibers is chemical vapor deposition (CVD; [25]). These carbon nanofibers can be further combined with other carbon nanoparticles, mainly graphene. For example, a composite paper consisting of nitrogen-doped carbon nanofibers, reduced graphene oxide (rGO) and bacterial cellulose was designed as a high-performance, mechanically tough, and bendable electrode for a supercapacitor. The bacterial nanocellulose in this paper is exploited both as a biomass precursor for the creation of carbon nanofibers by pyrolysis and as a supporting substrate for the newly-created material [21]. In another study, highly conductive freestanding cross-linked carbon nanofibers, derived from bacterial cellulose in a rapid plasma pyrolysis process, were used as substrates for the growth of vertically-oriented graphene sheets for constructing alternating current filtering supercapacitors [23]. A small amount of rGO can also act as an effective initiator of carbonization of cellulose nanofibers through microwave treatment [24]. Carbonization of aerogels, prepared from a mixture of PVA, cellulose nanofibers and GO by freeze-drying, enhanced the hydrophobic properties, the specific surface area and the adsorption capacity of these aerogels. These materials then became suitable candidates for oil-water separation and environmental protection [22]. In addition to graphene, cellulose-derived carbon nanofibers can be combined with various other nanoparticles and nanostructures, such as Pt nanoparticles for methanol oxidation reaction [161], TiO_2 films and Fe_3O_4 nanoparticles for lithium ion batteries [162], tin oxide (SnO) nanoparticles for lithium-sulfur batteries [163] or $NiCo_2S_4$ nanoparticles for hydrogen evolution reaction [164]. Carbon nanofibers are also promising for biomedical applications, particularly bone tissue engineering. Their nanoscale diameter produced a nanoscale surface roughness of their compacts or of their composite with poly-lactic-*co*-glycolic acid (PLGA). This nanoroughness promoted preferential adhesion of osteoblasts from other cell types, particularly fibroblasts, which could prevent fibrous encapsulation of bone implants [25].

6.2. Composites of Nanocellulose and Carbon Quantum Dots

Carbon quantum dots (CQDs) are quasispherical carbon nanoparticles (less than 10 nm in diameter) with a chemical structure and physical properties similar to those of graphene oxide. These nanoparticles emit a strong wavelength-dependent fluorescence. By changing the CQD size, the color of the emitted light can be tuned from deep ultraviolet to visible and near-infrared light. In addition, the fluorescence of CQDs, and also their water solubility, can be further modulated by functionalizing their surface with various atoms, chemical functional groups and molecules, such as metals, carboxyl groups, organic dyes and polymers. CQDs present good photostability, low photobleaching and relatively low cytotoxicity, and they are therefore considered to be suitable for biomedical applications such as bioimaging, biosensing, photodynamic and photothermal therapy of cancer, and drug delivery [165].

In hybrid materials with nanocellulose, CQDs were applied for constructing biosensors and drug delivery systems, and also for water purification. An optical sensor for visual discrimination of biothiols was based on a bacterial cellulose nanopaper substrate with ratiometric fluorescent sensing elements. These elements included N-acetyl l-cysteine capped green cadmium telluride (CdTe) quantum dots-rhodamine B and red CdTe quantum dots-carbon dots [26]. Hybrid materials containing carbon quantum dots and cellulose are also promising carriers for drug delivery. Composite core/shell chitosan-poly (ethylene oxide)-carbon quantum dots/carboxymethyl cellulose-poly(vinyl alcohol) nanofibers were prepared through coaxial electrospinning as a biodegradable implant for local delivery of temozolomide (TMZ), an anticancer drug. When tested in vitro, the antitumor activity of TMZ conjugated with carbon quantum dots against the tumor U251 cell lines was higher than the activity of the free drug [28]. Last but not least, carbon quantum dots, homogeneously dispersed together with magnetic Fe_3O_4 nanoparticles in electrospun cellulose nanofibers, were promising for the removal of Hg(II) ions from water [27].

6.3. Composites of Nanocellulose and Activated Carbon

Activated carbon is a form of carbon processed to have small, low-volume pores that increase the surface area, which is then available for the adsorption and removal of various toxic contaminants and microorganisms. Composite membranes consisting of a bilayer of porous activated carbon and TEMPO-oxidized plant-derived CNFs showed high capability for removing *Escherichia coli* from water [29]. Activated carbon was also a component of a wound dressing material consisting of a polyvinyl alcohol and cellulose acetate phthalate polymeric composite film, reinforced with Cu/Zn bimetal-dispersed activated carbon micro/nanofibers. This material suppressed the growth of *Pseudomonas aeruginosa*, the most prevalent bacteria in infected wounds caused by burns, surgery and traumatic injuries [30].

6.4. Composites of Nanocellulose and Carbon Black

Carbon black is a form of paracrystalline carbon, produced industrially by partial combustion or thermal decomposition of gaseous or liquid hydrocarbons under controlled conditions. Carbon black has a high surface-area-to-volume ratio, though not so high as that of activated carbon. Although it is considered to have low toxicity, the International Agency for Research on Cancer has classified it as possibly carcinogenic to humans. In addition, as a component of environmental pollution, carbon black can cause oxidative damage and an inflammatory reaction, which further mediate genotoxicity, reproductive toxicity, neurotoxicity and diseases of the respiratory and cardiovascular systems [166,167]. Nevertheless, carbon black is currently used as a filler in tires and in other rubber products, and as a pigment in inks, paints and plastics.

Composites of nanocellulose and carbon black have been used mainly for constructing biosensors, particularly wearable sensors for strain and human body motion, e.g., motion of the fingers, the elbow joint and the throat. A strain-sensing device with excellent waterproof, self-cleaning and anticorrosion properties was based on a superhydrophobic electrically conductive paper. This paper fabricated by dip-coating a printing paper into a carbon black/carbon nanotube/methyl cellulose suspension and into a hydrophobic fumed silica suspension [33]. Another strain-sensing device was fabricated by printing carbon black conductive nanostructures on cellulose acetate paper. At the same time, this material had electrochemical properties promising for the detection of hydrogen peroxide [31]. An electrochemical aptasensor for detecting *Staphylococcus aureus*, e.g., in human blood serum, was designed as a nanocomposite of Au nanoparticles, carbon black nanoparticles and cellulose nanofibers, and was endowed with a thiolated specific *S. aureus* aptamer as a sensing element [32].

7. Potential Cytotoxicity and Immunogenicity of Nanocellulose/Nanocarbon Composites

The vast majority of studies dealing with potential biomedical applications of nanocellulose/nanocarbon composites have reported no cytotoxicity or negligible cytotoxicity

of these composites, namely of nanocellulose/fullerene composites [35], nanocellulose/graphene composites [68,69,72,87,107], nanocellulose/CNT composites [51,149] and nanocellulose/nanodiamond composites [58,62,97]. Composites containing other carbon nanoparticles, such as activated carbon nanoparticles [30] or carbon quantum dots [28] have also shown no significant cytotoxic effects. In the mentioned studies, cytotoxicity was mainly tested in vitro on various cell types, such as fibroblasts, epithelial and endothelial cells, and mainly on cell lines, including tumor cell lines. The cell viability and proliferation were usually evaluated by tests of the activity of mitochondrial enzymes, such as MTT assay, resazurin (Alamar Blue) assay, or by a direct microscopic examination of the cells. Some composites have also been tested in vivo, e.g., in a rat model (nanocellulose/CNT composites; [106]), a canine model (nanocellulose/CNT composites; [52]), or using a chick chorioallantoic membrane model (nanocellulose/graphene composites, [107]), without adverse effects.

However, the individual components of nanocellulose/nanocarbon composites, particularly carbon nanoparticles, can act as cytotoxic, if they are not bound to any matrix and are free to move. Graphene and graphene-based carbon nanomaterials, such as fullerenes and nanotubes, are hydrophobic in their pristine state, and can enter into hydrophobic interactions with cholesterol in the cell membrane, which can be extracted from the membrane. In this manner, carbon nanoparticles can damage cells even without penetrating them. Another mechanism of cell membrane damage is the generation of reactive oxygen species (ROS) by carbon nanoparticles. In addition, the nanoparticles can penetrate the cell membrane, and can cause oxidative damage to mitochondria, and can also enter the cell nucleus and act as genotoxic agents (for a review, see [10,12,19,20]). Nanodiamonds have been considered to be relatively nontoxic in comparison with other carbon nanoparticles. However, as shown in our earlier studies, hydrophobic, hydrogen-terminated and positively-charged diamond nanoparticles can enter the cells, impair their growth and cause cell death [152,156]. The mechanism of cell damage by nanodiamonds is by generating ROS, and by excessive delivery of sodium ions adsorbed on the nanodiamond surface [168]. Last but not least, carbon nanoparticles can be immunogenic, i.e., they can activate inflammatory reactions, which can be, as has been demonstrated on carbon black, the main pathogenic mechanism of respiratory, cardiovascular and other serious diseases [166,167].

Cellulose nanoparticles, which are generally considered to be biocompatible [34,114] and of a low ecological toxicity [169], can also act as cytotoxic and immunogenic. It has even been speculated that, due to their high aspect ratio and stiffness, CNCs may cause similar pulmonary toxicity as carbon nanotubes and asbestos [170]. In a mouse model, cellulose nanocrystals induced oxidative stress, caused pulmonary inflammation and damage, increased levels of collagen and transforming growth factor-beta (TGF-β) in lungs, and impaired pulmonary functions [170]. In addition, these effects were markedly more pronounced in female mice than in male mice. The immunogenicity of CNCs was also proven in vitro. CNCs and their cationic derivatives CNC-aminoethylmethacrylate and CNC-aminoethylmethacrylamide evoked an inflammatory response in mouse macrophage J774A.1 cells and in peripheral blood mononuclear cells by increasing the level of ROS in mitochondria, the release of ATP from mitochondria and by stimulating the secretion of interleukin-1beta (IL-1β) [171]. The cytotoxicity and immunogenicity of CNCs depend on the preparation conditions and are increased under harsh and caustic conditions, e.g., the so-called mercerization process, i.e., an alkali treatment [149]. CNFs can also cause cytotoxicity and oxidative damage, which can be even more pronounced than in the case of CNCs, and can evoke an inflammatory response (for a review, see [2,172]). The potential cytotoxicity and immunogenicity of nanocellulose, nanocarbon and their composites should therefore be taken into account when they are for use in biomedical applications.

8. Conclusions

Nanocellulose/nanocarbon composites and other hybrid materials containing cellulose nanoparticles (nanofibrils or nanocrystals) and carbon nanoparticles (fullerenes, graphene, carbon nanotubes, nanodiamonds and other carbon nanoparticles) are novel materials that are promising for a wide range of applications in industry, (bio)technology and medicine. This is due to their unique

properties, such as high mechanical strength coupled with flexibility and stretchability (composites with graphene, carbon nanotubes and nanodiamond), shape memory (composites with graphene and carbon nanotubes), photodynamic and photothermal activity (composites with fullerenes and graphene), electrical conductivity (composites with graphene and carbon nanotubes), semiconductivity (composites with boron-doped diamond), thermal conductivity (composites with graphene and nanodiamonds), tunable optical transparency (composites with single-walled carbon nanotubes and nanodiamonds), intrinsic fluorescence and luminescence (composites with graphene quantum dots and carbon quantum dots), and high adsorption and filtration capacity (composites with graphene, carbon nanotubes and carbon quantum dots). These properties arise mainly from the advantageous combination of nanocellulose and nanocarbon, which associates and enhances the desirable effects of each of these components. These materials can be prepared relatively easily from a water-based suspension, which is advantageous particularly for biomedical applications. These applications include drug delivery, biosensorics, isolation of various biomolecules, electrical stimulation of damaged tissues, and particularly tissue engineering (bone, neural and vascular) and wound dressing. Our results have proven supportive effects of nanocellulose/carbon nanotube composites on the adhesion and growth of human and porcine adipose tissue-derived stem cells, particularly under dynamic cultivation in a pressure-generating lab-made bioreactor (see Appendix A). However, it should be pointed out that the biomedical applications of nanocellulose/nanocarbon composites are associated with the risk of their potential cytotoxicity and immunogenicity, although this risk appears to be lower than for the single components of these materials.

Author Contributions: All authors have read and agree to the published version of the manuscript. Conceptualization, L.B., S.S. and A.S.; methodology, J.P., M.T., R.M., J.S., S.P., A.S., S.S.; software, R.M., J.S., A.B.; validation, L.B., R.M.; formal analysis, L.B., A.B., A.S., S.S.; investigation, J.P., M.T., R.M., J.S., S.P., A.S., S.S.; resources, L.B., P.K.; data curation, J.P., R.M., A.B., A.S.; writing—original draft preparation, L.B., J.P., R.M.; writing—review and editing, A.B., A.S., S.S., P.K.; visualization, J.P., M.T., R.M., A.B.; supervision, L.B., P.K.; project administration, L.B.; funding acquisition, L.B.

Funding: This research was funded by the Czech Science Foundation (grant no. 17-00885S). Another support was provided by the BIOCEV – Biotechnology and Biomedicine Centre of the Academy of Sciences and Charles University project (CZ.1.05/1.1.00/02.0109), funded by the European Regional Development Fund.

Acknowledgments: Robin Healey (Czech Technical University, Prague) is gratefully acknowledged for his language revision of the manuscript. Panu Lahtinen from VTT (Technical Research Center of Finland, Espoo, Finland) is acknowledged for providing nanocellulose for collaborative work between Tampere University of Technology and Institute of Physiology of the Czech Academy of Sciences.

Conflicts of Interest: The authors declare no conflict of interest. The funding sponsors had no role in the design of the study; in the collection, analyses, or interpretation of data; in the writing of the manuscript, and in the decision to publish the results.

Appendix A

In our own experiments, we have contributed to the knowledge on potential biomedical applications of nanocellulose/carbon nanotube composites, namely regarding their application in tissue engineering. In these experiments, a PurCotton® cellulose mesh (Winner Industrial Park, Shenzhen, China) was modified with an aqueous dispersion of positively-charged (i.e., cationic) wood-derived CNFs, described in our earlier review article [2], and MWCNTs. Two types of composite samples were prepared, namely the samples with "thick" and "thin" coating of the fibers in the cellulose mesh. For thick coating, square-shaped samples of the cellulose mesh were fully immersed in an aqueous suspension of CNFs+MWCNTs, and during this immersion, the samples were homogeneously impregnated with the nanoparticles. For thin coating, only one corner of the cellulose samples was submerged into the CNF+MWCNT suspension, which resulted in infiltration of the suspension throughout the cellulose mesh by capillary forces. Both types of samples were then dried for 5 h at 60 °C. Both types of samples displayed a grayish color, which was more intense in samples with a thick coating. A pure CNF coating was prepared similarly to the thick coatings, and the meshes without coating were used as a control.

The samples were sterilized by UV light (20 min for each side), fixed into CellCrowns™ inserts (Scaffdex Ltd., Tampere, Finland), placed into 24-well cell culture plates (TPP, Trasadingen, Switzerland) and seeded with human adipose tissue-derived stem cells (hASC) or porcine adipose tissue-derived stem cells (pASC). Human ASC were isolated from subcutaneous fat tissue, obtained by liposuction from the abdominal region of healthy female donors after their informed consent, under ethical approval issued by the Ethics Committee of Hospital "Na Bulovce" in Prague, and in compliance with the tenets of the Declaration of Helsinki on experiments involving human tissues. The isolation was described in more details in our earlier studies [173,174]. Porcine ASC were isolated by enzymatic disintegration of subcutaneous fat tissue samples obtained by excision from laboratory pigs in collaboration with the Institute of Clinical and Experimental Medicine (IKEM) in Prague, Czech Republic. Characterization of cells by flow cytometry revealed the positivity of cells for standard surface markers of ASCs, namely CD105, CD90, CD73 and CD29 in hASC, and CD105, CD90, CD29 and CD44 in pASCs. The ASCs from both species were negative or almost negative for hematopoietic markers, such as CD34 and CD45, and for CD31, an endothelial marker [174,175].

The cells were seeded on the material samples at a density of 50,000 cells per well into 1.5 mL of the culture media. Human ASCs were cultivated in Dulbecco's modified Eagle's Medium (DMEM; Life Technologies, Gibco, Carlsbad, CA, USA) with 10% of fetal bovine serum (FBS; Life Technologies, Gibco), 40 μg/mL of gentamicin (LEK, Ljubljana, Slovenia) and 10 ng/mL of recombinant human fibroblast growth factor basic (FGF2; GenScript, Piscataway, NJ, USA). Porcine ASCs were cultivated in Dulbecco's modified Eagle's Medium (Low glucose, Sigma-Aldrich Co., St. Louis, MO, USA) and Ham's Nutrient Mixture F12 medium (DMEM/F 12, Sigma-Aldrich Co.) in a ratio of 1:1 with 10% of fetal bovine serum (FBS; Life Technologies, Gibco), 1% Antibiotic Antimycotic solution (Sigma-Aldrich Co.) and 10 ng/mL of recombinant human fibroblast growth factor basic (FGF2; GenScript).

After one or seven days of cultivation, the cells were fixed with 4% paraformaldehyde (Sigma-Aldrich Co.) for 20 min, and 0.1% Triton X-100 (Sigma-Aldrich Co.) diluted in phosphate-buffered saline (PBS) was applied for 20 min at room temperature in order to permeabilize the cell membranes. Nonspecific binding sites for antibodies were then blocked by a solution of 1% bovine serum albumin and 0.1% Tween 20 in PBS (all Sigma-Aldrich Co.). Vinculin, a protein of focal adhesion plaques associated with integrin adhesion receptors, was visualized by treating the samples for 1 h at 37 °C with primary antibody against human vinculin (V9131, monoclonal mouse antibody, clone hVIN-1, Sigma-Aldrich Co.), diluted in the blocking solution (1% albumin and 0.1% Tween 20 in PBS) in a ratio of 1:200. After washing with PBS, the samples were incubated for 1 h at room temperature in the dark with a secondary antibody, i.e., goat anti-mouse F(ab')2 fragments of IgG (H + L), conjugated with Alexa Fluor® 488 (A11017; Molecular Probes, Eugene, OR, USA; Thermo Fisher Scientific, Waltham, MA, USA), diluted in PBS to a ratio of 1:400. Finally, cytoskeletal F-actin filaments were stained by phalloidin conjugated with tetramethylrhodamine isothiocynate (TRITC) fluorescent dye (Sigma-Aldrich Co.), diluted in PBS to a final concentration of 5 μg/mL, for 1 h at room temperature in the dark. Microscopy images were acquired using spinning disk confocal system Dragonfly 503 (Andor, Belfast, UK) with Zyla 4.2 PLUS sCMOS camera (Andor, Belfast, UK) mounted on microscope Leica DMi8 (Leica Microsystems, Wetzlar, Germany) with objective HC PL APO 20x/0.75 IMM CORR CS2; Free Working Distance = 0.66 mm or HC PL APO 40x/1.10 W CORR CS2; Free Working Distance = 0.65 mm.

We found that the initial adhesion and subsequent growth of cells, evaluated by the cell number and spreading on days 1 and 7, were similar on all coated samples. There was no apparent difference between samples coated with thick and thin layers of CNFs + MWCNTs and samples coated only with CNFs. However, all types of coatings markedly improved the adhesion and growth of cells in comparison with a pure uncoated cellulose mesh (Figure A1). In general, the cell growth was relatively slow in all tested samples. On day 7, the cell number in all tested samples was only slightly higher than on day 1. In addition, hASCs grew slightly better than pASCs, particularly on samples coated with CNFs+MWCNTs. Therefore, we decided to cultivate pASCs on the tested samples under dynamic

conditions, which are known to improve the growth of cells by their mechanical stimulation, by a better supply of nutrients and oxygen and by quicker waste removal.

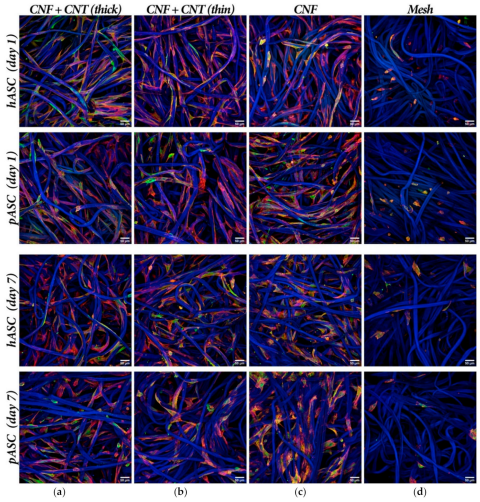

Figure A1. Human adipose tissue-derived stem cells (hASC) and porcine adipose tissue-derived stem cells (pASC) on days 1 and 7 after seeding on a cellulose mesh with thick or thin CNF+MWCNT coating (column (**a**) and (**b**), respectively), with CNF coating (column (**c**)), and without any coating (column (**d**)). Cells were stained by immunofluorescence for vinculin (green), with TRITC-conjugated phalloidin for F-actin (red) and with Hoechst #33258 for the nuclei (blue). Cellulose mesh had autofluorescence in the blue channel. Dragonfly 503 spinning disk confocal microscope with a Zyla 4.2 PLUS sCMOS camera, objective HC PL APO 20x/0.75 IMM CORR CS2. Scale bar: 50 µm.

The dynamic cultivation was held in a unique lab-made cultivation chamber (Figure A2). This chamber allows for fixing a standard well plate with tested substrates and its hermetical sealing to maintain the desired pressure. This chamber was connected to a custom pressure stimulator. This stimulator consists of a servo-controlled linear stage with piston pump and special controlling software. This software allows for setting stimulation parameters that include high/low pressure, motor speed, pulsatile frequency and the shape of the pressure wave.

Porcine ASCs were seeded on CellCrown-fixed substrates in 24-well plates at the same number and in the same cultivation medium as mentioned above. Afterwards, the well plate for dynamic cultivation was fixed into the cultivation chamber, and this chamber was sealed and connected to the pressure stimulator. In the initial phase, the cells were left for 24 h without any pressure stimulation in order to allow their adhesion to the materials. The system was opened through a 220-nm filter to atmosphere forced with slow motion of pump piston to equilibrate CO_2 level and pH of medium. After this resting phase, the pressure stimulation was set to 15.9/10.6 kPa (120/80 mmHg) high/low pressure with frequency of 1 Hz (60 pulses per minute) with triangular pulse shape with 1:1 ratio. This dynamic cultivation lasted for 72 h (96 h of cultivation in total including the 24-h rest phase). Static control samples were cultivated for 96 h in a well plate with standard lid in the same CO_2 incubator as the dynamic samples.

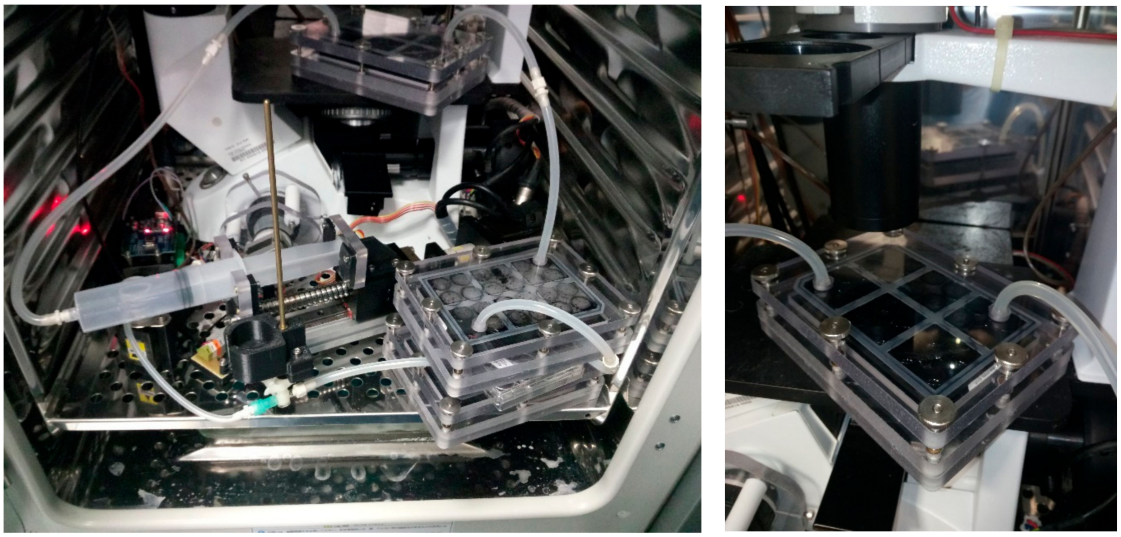

(**a**) (**b**)

Figure A2. Lab-made dynamic cultivation system for pressure stimulation of cells on the tested material samples. The whole system in a cell incubator (**a**); detail of a cultivation chamber (**b**).

We found that dynamic cell cultivation markedly improved the adhesion and subsequent growth of pASCs. The cells were better spread and their number after three days of dynamic cultivation (day 4 after seeding) was markedly higher than in the corresponding samples incubated under static conditions for four days (Figure A3), and also for seven days (Figure A1). The improvement in cell colonization by dynamic cultivation was observed particularly on samples with thin CNF + MWCNT coating. On both thick and thin CNF + MWCNT coatings, the cells under dynamic conditions were distributed almost homogeneously, while on the pure CNF coating, the cells tended to form clusters. A similar picture was observed in our earlier study performed on human dermal fibroblasts in four-day-old static cultures on the same cationic CNFs, where the cells were less widespread and distributed less homogeneously than on anionic CNFs [2]. Therefore, it can be concluded that the addition of MWCNTs to cationic CNFs improved the colonization of the material with pASCs under dynamic cell culture conditions.

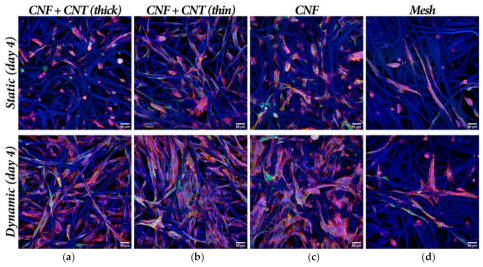

Figure A3. Porcine adipose tissue-derived stem cells (pASC) cultivated in a conventional static cell culture system for four days or in a pressure-generating dynamic cell culture system for three days (after one day of static cultivation). The cells were grown on a cellulose mesh with thick or thin CNF + MWCNT coating (column (**a**) and (**b**), respectively), with CNF coating (column (**c**)), and without any coating (column (**d**)). Cells were stained by immunofluorescence for vinculin (green), with TRITC-conjugated phalloidin for F-actin (red) and with DAPI for the nuclei (blue). Cellulose mesh had autofluorescence in the blue channel. Dragonfly 503 spinning disk confocal microscope with a Zyla 4.2 PLUS sCMOS camera, objective HC PL APO 20x/0.75 IMM CORR CS2. Scale bar: 50 µm.

References

1. Zhang, H.; Dou, C.; Pal, L.; Hubbe, M.A. Review of Electrically Conductive Composites and Films Containing Cellulosic Fibers or Nanocellulose. *Bioresources* **2019**, 14.
2. Bacakova, L.; Pajorova, J.; Bacakova, M.; Skogberg, A.; Kallio, P.; Kolarova, K.; Svorcik, V. Versatile Application of Nanocellulose: From Industry to Skin Tissue Engineering and Wound Healing. *Nanomaterials (Basel)* **2019**, *9*, 164. [CrossRef] [PubMed]
3. Zhang, Y.X.; Nypelo, T.; Salas, C.; Arboleda, J.; Hoeger, I.C.; Rojas, O.J. Cellulose Nanofibrils: From Strong Materials to Bioactive Surfaces. *J Renew Mater* **2013**, *1*, 195–211. [CrossRef]
4. Lin, N.; Dufresne, A. Nanocellulose in biomedicine: Current status and future prospect. *Eur Polym J* **2014**, *59*, 302–325. [CrossRef]
5. Bhattacharya, M.; Malinen, M.M.; Lauren, P.; Lou, Y.R.; Kuisma, S.W.; Kanninen, L.; Lille, M.; Corlu, A.; GuGuen-Guillouzo, C.; Ikkala, O.; et al. Nanofibrillar cellulose hydrogel promotes three-dimensional liver cell culture. *J Control Release* **2012**, *164*, 291–298. [CrossRef]
6. Lou, Y.R.; Kanninen, L.; Kuisma, T.; Niklander, J.; Noon, L.A.; Burks, D.; Urtti, A.; Yliperttula, M. The Use of Nanofibrillar Cellulose Hydrogel As a Flexible Three-Dimensional Model to Culture Human Pluripotent Stem Cells. *Stem Cells Dev* **2014**, *23*, 380–392. [CrossRef]
7. Julkapli, N.M.; Bagheri, S. Nanocellulose as a green and sustainable emerging material in energy applications: a review. *Polym Advan Technol* **2017**, *28*, 1583–1594. [CrossRef]
8. *Nanotechnologies — Standard terms and their definition for cellulose nanomaterial. ISO/TS 20477:2017(E)*, 1st ed.; ISO/TS 20477:2017; ISO: Vernier, Switzerland; Geneva, Switzerland, 2017.
9. Habibi, Y.; Lucia, L.A.; Rojas, O.J. Cellulose Nanocrystals: Chemistry, Self-Assembly, and Applications. *Chem Rev* **2010**, *110*, 3479–3500. [CrossRef] [PubMed]
10. Bacakova, L.; Grausova, L.; Vandrovcova, M.; Vacik, J.; Frazcek, A.; Blazewicz, S.; Kromka, A.; Vanecek, M.; Nesladek, M.; Svorcik, V.; et al. Carbon nanoparticles as substrates for cell adhesion and growth. In *Nanoparticles: New Research*; Lombardi, S.L., Ed.; Nova Science Publishers, Inc.: Hauppauge, NY, USA, 2008; pp. 39–107. ISBN 978-1-60456-704-5.
11. Bacakova, L.; Grausova, L.; Vacik, J.; Kromka, A.; Biederman, H.; Choukourov, A.; Stary, V. Nanocomposite and nanostructured carbon-based films as growth substrates for bone cells. In *Advances in Diverse Industrial Applications of Nanocomposites*; Reddy, B., Ed.; IntechOpen: London, UK, 2011; pp. 399–435. ISBN 978-953-307-202-9.
12. Bacakova, L.; Kopova, I.; Vacik, J.; Lavrentiev, V. Interaction of fullerenes and metal-fullerene composites with cells. In *Fullerenes: Chemistry, Natural Sources and Technological Applications*; Ellis, S.B., Ed.; Nova Science Publishers, Inc.: Hauppauge, NY, USA, 2014; pp. 1–33.
13. Bacakova, L.; Kopova, I.; Stankova, L.; Liskova, J.; Vacik, J.; Lavrentiev, V.; Kromka, A.; Potocky, S.; Stranska, D. Bone cells in cultures on nanocarbon-based materials for potential bone tissue engineering: A review. *Phys Status Solidi A* **2014**, *211*, 2688–2702. [CrossRef]
14. Bacakova, L.; Filova, E.; Liskova, J.; Kopova, I.; Vandrovcova, M.; Havlikova, J. Nanostructured materials as substrates for the adhesion, growth, and osteogenic differentiation of bone cells. *Appl Nanobiomater* **2016**, *4*, 103–153. [CrossRef]
15. Bacakova, L.; Broz, A.; Liskova, J.; Stankova, L.; Potocky, S.; Kromka, A. Application of nanodiamond in biotechnology and tissue engineering. In *Diamond and Carbon Composites and Nanocomposites*; Aliofkhazraei, M., Ed.; IntechOpen: London, UK, 2016; pp. 59–88. ISBN 978-953-51-2453-5. [CrossRef]
16. Wong, B.S.; Yoong, S.L.; Jagusiak, A.; Panczyk, T.; Ho, H.K.; Ang, W.H.; Pastorin, G. Carbon nanotubes for delivery of small molecule drugs. *Adv Drug Deliv Rev* **2013**, *65*, 1964–2015. [CrossRef] [PubMed]
17. Wang, M.; Anoshkin, I.V.; Nasibulin, A.G.; Korhonen, J.T.; Seitsonen, J.; Pere, J.; Kauppinen, E.I.; Ras, R.H.; Ikkala, O. Modifying native nanocellulose aerogels with carbon nanotubes for mechanoresponsive conductivity and pressure sensing. *Adv Mater* **2013**, *25*, 2428–2432. [CrossRef] [PubMed]
18. Yin, R.; Agrawal, T.; Khan, U.; Gupta, G.K.; Rai, V.; Huang, Y.Y.; Hamblin, M.R. Antimicrobial photodynamic inactivation in nanomedicine: small light strides against bad bugs. *Nanomedicine (Lond)* **2015**, *10*, 2379–2404. [CrossRef] [PubMed]
19. Liao, C.; Li, Y.; Tjong, S.C. Graphene Nanomaterials: Synthesis, Biocompatibility, and Cytotoxicity. *Int J Mol Sci* **2018**, *19*, 3564. [CrossRef]

20. Placha, D.; Jampilek, J. Graphenic Materials for Biomedical Applications. *Nanomaterials (Basel)* **2019**, *9*, 1758. [CrossRef]
21. Ma, L.; Liu, R.; Niu, H.; Xing, L.; Liu, L.; Huang, Y. Flexible and Freestanding Supercapacitor Electrodes Based on Nitrogen-Doped Carbon Networks/Graphene/Bacterial Cellulose with Ultrahigh Areal Capacitance. *ACS Appl Mater Interfaces* **2016**, *8*, 33608–33618. [CrossRef]
22. Xu, Z.; Zhou, H.; Tan, S.; Jiang, X.; Wu, W.; Shi, J.; Chen, P. Ultralight super-hydrophobic carbon aerogels based on cellulose nanofibers/poly(vinyl alcohol)/graphene oxide (CNFs/PVA/GO) for highly effective oil-water separation. *Beilstein J Nanotechnol* **2018**, *9*, 508–519. [CrossRef]
23. Li, W.; Islam, N.; Ren, G.; Li, S.; Fan, Z. AC-Filtering Supercapacitors Based on Edge Oriented Vertical Graphene and Cross-Linked Carbon Nanofiber. *Materials (Basel)* **2019**, *12*, 604. [CrossRef]
24. Shi, Q.; Liu, D.; Wang, Y.; Zhao, Y.; Yang, X.; Huang, J. High-Performance Sodium-Ion Battery Anode via Rapid Microwave Carbonization of Natural Cellulose Nanofibers with Graphene Initiator. *Small* **2019**, *15*, e1901724. [CrossRef]
25. Price, R.L.; Ellison, K.; Haberstroh, K.M.; Webster, T.J. Nanometer surface roughness increases select osteoblast adhesion on carbon nanofiber compacts. *J Biomed Mater Res A* **2004**, *70*, 129–138. [CrossRef]
26. Abbasi-Moayed, S.; Golmohammadi, H.; Bigdeli, A.; Hormozi-Nezhad, M.R. A rainbow ratiometric fluorescent sensor array on bacterial nanocellulose for visual discrimination of biothiols. *Analyst* **2018**, *143*, 3415–3424. [CrossRef]
27. Li, L.; Wang, F.; Lv, Y.; Liu, J.; Bian, H.; Wang, W.; Li, Y.; Shao, Z. CQDs-Doped Magnetic Electrospun Nanofibers: Fluorescence Self-Display and Adsorption Removal of Mercury(II). *ACS Omega* **2018**, *3*, 4220–4230. [CrossRef] [PubMed]
28. Shamsipour, M.; Mansouri, A.M.; Moradipour, P. Temozolomide Conjugated Carbon Quantum Dots Embedded in Core/Shell Nanofibers Prepared by Coaxial Electrospinning as an Implantable Delivery System for Cell Imaging and Sustained Drug Release. *AAPS PharmSciTech* **2019**, *20*, 259. [CrossRef] [PubMed]
29. Hassan, M.; Abou-Zeid, R.; Hassan, E.; Berglund, L.; Aitomaki, Y.; Oksman, K. Membranes Based on Cellulose Nanofibers and Activated Carbon for Removal of Escherichia coli Bacteria from Water. *Polymers (Basel)* **2017**, *9*, 335. [CrossRef] [PubMed]
30. Ashfaq, M.; Verma, N.; Khan, S. Highly effective Cu/Zn-carbon micro/nanofiber-polymer nanocomposite-based wound dressing biomaterial against the P. aeruginosa multi- and extensively drug-resistant strains. *Mater Sci Eng C Mater Biol Appl* **2017**, *77*, 630–641. [CrossRef]
31. Santhiago, M.; Correa, C.C.; Bernardes, J.S.; Pereira, M.P.; Oliveira, L.J.M.; Strauss, M.; Bufon, C.C.B. Flexible and Foldable Fully-Printed Carbon Black Conductive Nanostructures on Paper for High-Performance Electronic, Electrochemical, and Wearable Devices. *ACS Appl Mater Interfaces* **2017**, *9*, 24365–24372. [CrossRef]
32. Ranjbar, S.; Shahrokhian, S. Design and fabrication of an electrochemical aptasensor using Au nanoparticles/carbon nanoparticles/cellulose nanofibers nanocomposite for rapid and sensitive detection of Staphylococcus aureus. *Bioelectrochemistry* **2018**, *123*, 70–76. [CrossRef]
33. Li, Q.M.; Liu, H.; Zhang, S.D.; Zhang, D.B.; Liu, X.H.; He, Y.X.; Mi, L.W.; Zhang, J.X.; Liu, C.T.; Shen, C.Y.; et al. Superhydrophobic Electrically Conductive Paper for Ultrasensitive Strain Sensor with Excellent Anticorrosion and Self-Cleaning Property. *Acs Appl Mater Inter* **2019**, *11*, 21904–21914. [CrossRef]
34. Lin, J.; Zhong, Z.; Li, Q.; Tan, Z.; Lin, T.; Quan, Y.; Zhang, D. Facile Low-Temperature Synthesis of Cellulose Nanocrystals Carrying Buckminsterfullerene and Its Radical Scavenging Property in Vitro. *Biomacromolecules* **2017**, *18*, 4034–4040. [CrossRef]
35. Herreros-Lopez, A.; Carini, M.; Da Ros, T.; Carofiglio, T.; Marega, C.; La Parola, V.; Rapozzi, V.; Xodo, L.E.; Alshatwi, A.A.; Hadad, C.; et al. Nanocrystalline cellulose-fullerene: Novel conjugates. *Carbohydr Polym* **2017**, *164*, 92–101. [CrossRef]
36. Kim, Y.; Kim, H.S.; Yun, Y.S.; Bak, H.; Jin, H.J. Ag-doped multiwalled carbon nanotube/polymer composite electrodes. *J Nanosci Nanotechnol* **2010**, *10*, 3571–3575. [CrossRef] [PubMed]
37. Jin, L.; Zeng, Z.; Kuddannaya, S.; Wu, D.; Zhang, Y.; Wang, Z. Biocompatible, Free-Standing Film Composed of Bacterial Cellulose Nanofibers-Graphene Composite. *ACS Appl Mater Interfaces* **2016**, *8*, 1011–1018. [CrossRef] [PubMed]
38. Kim, S.; Xiong, R.; Tsukruk, V.V. Probing Flexural Properties of Cellulose Nanocrystal-Graphene Nanomembranes with Force Spectroscopy and Bulging Test. *Langmuir* **2016**, *32*, 5383–5393. [CrossRef] [PubMed]

39. Siljander, S.; Keinanen, P.; Raty, A.; Ramakrishnan, K.R.; Tuukkanen, S.; Kunnari, V.; Harlin, A.; Vuorinen, J.; Kanerva, M. Effect of Surfactant Type and Sonication Energy on the Electrical Conductivity Properties of Nanocellulose-CNT Nanocomposite Films. *Int J Mol Sci* **2018**, *19*, 1819. [CrossRef] [PubMed]
40. Han, J.; Wang, S.; Zhu, S.; Huang, C.; Yue, Y.; Mei, C.; Xu, X.; Xia, C. Electrospun Core-Shell Nanofibrous Membranes with Nanocellulose-Stabilized Carbon Nanotubes for Use as High-Performance Flexible Supercapacitor Electrodes with Enhanced Water Resistance, Thermal Stability, and Mechanical Toughness. *ACS Appl Mater Interfaces* **2019**, *11*, 44624–44635. [CrossRef]
41. Nguyen, H.K.; Bae, J.; Hur, J.; Park, S.J.; Park, M.S.; Kim, I.T. Tailoring of Aqueous-Based Carbon Nanotube(-)Nanocellulose Films as Self-Standing Flexible Anodes for Lithium-Ion Storage. *Nanomaterials (Basel)* **2019**, *9*, 655. [CrossRef]
42. Jiang, M.; Seney, R.; Bayliss, P.C.; Kitchens, C.L. Carbon Nanotube and Cellulose Nanocrystal Hybrid Films. *Molecules* **2019**, *24*, 2662. [CrossRef]
43. Liu, P.; Zhu, C.; Mathew, A.P. Mechanically robust high flux graphene oxide - nanocellulose membranes for dye removal from water. *J Hazard Mater* **2019**, *371*, 484–493. [CrossRef]
44. Hasan, M.Q.; Yuen, J.; Slaughter, G. Carbon Nanotube-Cellulose Pellicle for Glucose Biofuel Cell. *Conf Proc IEEE Eng Med Biol Soc* **2018**, *2018*, 1–4. [CrossRef]
45. Hamedi, M.M.; Hajian, A.; Fall, A.B.; Hakansson, K.; Salajkova, M.; Lundell, F.; Wagberg, L.; Berglund, L.A. Highly conducting, strong nanocomposites based on nanocellulose-assisted aqueous dispersions of single-wall carbon nanotubes. *ACS Nano* **2014**, *8*, 2467–2476. [CrossRef] [PubMed]
46. Hajian, A.; Lindstrom, S.B.; Pettersson, T.; Hamedi, M.M.; Wagberg, L. Understanding the Dispersive Action of Nanocellulose for Carbon Nanomaterials. *Nano Lett* **2017**, *17*, 1439–1447. [CrossRef] [PubMed]
47. Hamedi, M.; Karabulut, E.; Marais, A.; Herland, A.; Nystrom, G.; Wagberg, L. Nanocellulose aerogels functionalized by rapid layer-by-layer assembly for high charge storage and beyond. *Angew Chem Int Ed Engl* **2013**, *52*, 12038–12042. [CrossRef] [PubMed]
48. Wicklein, B.; Kocjan, A.; Salazar-Alvarez, G.; Carosio, F.; Camino, G.; Antonietti, M.; Bergstrom, L. Thermally insulating and fire-retardant lightweight anisotropic foams based on nanocellulose and graphene oxide. *Nat Nanotechnol* **2015**, *10*, 277–283. [CrossRef] [PubMed]
49. Yousefi, N.; Wong, K.K.W.; Hosseinidoust, Z.; Sorensen, H.O.; Bruns, S.; Zheng, Y.; Tufenkji, N. Hierarchically porous, ultra-strong reduced graphene oxide-cellulose nanocrystal sponges for exceptional adsorption of water contaminants. *Nanoscale* **2018**, *10*, 7171–7184. [CrossRef] [PubMed]
50. Siljander, S.; Keinanen, P.; Ivanova, A.; Lehmonen, J.; Tuukkanen, S.; Kanerva, M.; Bjorkqvist, T. Conductive Cellulose based Foam Formed 3D Shapes-From Innovation to Designed Prototype. *Materials (Basel)* **2019**, *12*, 430. [CrossRef]
51. Kuzmenko, V.; Karabulut, E.; Pernevik, E.; Enoksson, P.; Gatenholm, P. Tailor-made conductive inks from cellulose nanofibrils for 3D printing of neural guidelines. *Carbohydr Polym* **2018**, *189*, 22–30. [CrossRef]
52. Pedrotty, D.M.; Kuzmenko, V.; Karabulut, E.; Sugrue, A.M.; Livia, C.; Vaidya, V.R.; McLeod, C.J.; Asirvatham, S.J.; Gatenholm, P.; Kapa, S. Three-Dimensional Printed Biopatches With Conductive Ink Facilitate Cardiac Conduction When Applied to Disrupted Myocardium. *Circ Arrhythm Electrophysiol* **2019**, *12*, e006920. [CrossRef]
53. Shah, N.; Ul-Islam, M.; Khattak, W.A.; Park, J.K. Overview of bacterial cellulose composites: a multipurpose advanced material. *Carbohydr Polym* **2013**, *98*, 1585–1598. [CrossRef]
54. Xu, T.; Jiang, Q.; Ghim, D.; Liu, K.K.; Sun, H.; Derami, H.G.; Wang, Z.; Tadepalli, S.; Jun, Y.S.; Zhang, Q.; et al. Catalytically Active Bacterial Nanocellulose-Based Ultrafiltration Membrane. *Small* **2018**, *14*, e1704006. [CrossRef]
55. Jun, Y.S.; Wu, X.; Ghim, D.; Jiang, Q.; Cao, S.; Singamaneni, S. Photothermal Membrane Water Treatment for Two Worlds. *Acc Chem Res* **2019**, *52*, 1215–1225. [CrossRef]
56. Jiang, Q.; Ghim, D.; Cao, S.; Tadepalli, S.; Liu, K.K.; Kwon, H.; Luan, J.; Min, Y.; Jun, Y.S.; Singamaneni, S. Photothermally Active Reduced Graphene Oxide/Bacterial Nanocellulose Composites as Biofouling-Resistant Ultrafiltration Membranes. *Environ Sci Technol* **2019**, *53*, 412–421. [CrossRef] [PubMed]
57. Abol-Fotouh, D.; Dorling, B.; Zapata-Arteaga, O.; Rodriguez-Martinez, X.; Gomez, A.; Reparaz, J.S.; Laromaine, A.; Roig, A.; Campoy-Quiles, M. Farming thermoelectric paper. *Energy Environ Sci* **2019**, *12*, 716–726. [CrossRef] [PubMed]

58. Mahdavi, M.; Mahmoudi, N.; Rezaie Anaran, F.; Simchi, A. Electrospinning of Nanodiamond-Modified Polysaccharide Nanofibers with Physico-Mechanical Properties Close to Natural Skins. *Mar Drugs* **2016**, *14*, 128. [CrossRef] [PubMed]
59. Liu, X.; Shen, H.; Song, S.; Chen, W.; Zhang, Z. Accelerated biomineralization of graphene oxide - incorporated cellulose acetate nanofibrous scaffolds for mesenchymal stem cell osteogenesis. *Colloids Surf B Biointerfaces* **2017**, *159*, 251–258. [CrossRef] [PubMed]
60. Cho, S.Y.; Yu, H.; Choi, J.; Kang, H.; Park, S.; Jang, J.S.; Hong, H.J.; Kim, I.D.; Lee, S.K.; Jeong, H.S.; et al. Continuous Meter-Scale Synthesis of Weavable Tunicate Cellulose/Carbon Nanotube Fibers for High-Performance Wearable Sensors. *ACS Nano* **2019**, *13*, 9332–9341. [CrossRef] [PubMed]
61. Zhu, C.; Liu, P.; Mathew, A.P. Self-Assembled TEMPO Cellulose Nanofibers: Graphene Oxide-Based Biohybrids for Water Purification. *ACS Appl Mater Interfaces* **2017**, *9*, 21048–21058. [CrossRef] [PubMed]
62. Ostadhossein, F.; Mahmoudi, N.; Morales-Cid, G.; Tamjid, E.; Navas-Martos, F.J.; Soriano-Cuadrado, B.; Paniza, J.M.L.; Simchi, A. Development of Chitosan/Bacterial Cellulose Composite Films Containing Nanodiamonds as a Potential Flexible Platform for Wound Dressing. *Materials (Basel)* **2015**, *8*, 6401–6418. [CrossRef]
63. Zheng, C.; Yue, Y.; Gan, L.; Xu, X.; Mei, C.; Han, J. Highly Stretchable and Self-Healing Strain Sensors Based on Nanocellulose-Supported Graphene Dispersed in Electro-Conductive Hydrogels. *Nanomaterials (Basel)* **2019**, *9*, 937. [CrossRef]
64. Xing, J.; Tao, P.; Wu, Z.; Xing, C.; Liao, X.; Nie, S. Nanocellulose-graphene composites: A promising nanomaterial for flexible supercapacitors. *Carbohydr Polym* **2019**, *207*, 447–459. [CrossRef]
65. Shi, Z.; Phillips, G.O.; Yang, G. Nanocellulose electroconductive composites. *Nanoscale* **2013**, *5*, 3194–3201. [CrossRef]
66. Buzid, A.; Hayes, P.E.; Glennon, J.D.; Luong, J.H.T. Captavidin as a regenerable biorecognition element on boron-doped diamond for biotin sensing. *Anal Chim Acta* **2019**, *1059*, 42–48. [CrossRef] [PubMed]
67. Li, F.; Yu, H.Y.; Wang, Y.Y.; Zhou, Y.; Zhang, H.; Yao, J.M.; Abdalkarim, S.Y.H.; Tam, K.C. Natural Biodegradable Poly(3-hydroxybutyrate-co-3-hydroxyvalerate) Nanocomposites with Multifunctional Cellulose Nanocrystals/Graphene Oxide Hybrids for High-Performance Food Packaging. *J Agric Food Chem* **2019**, *67*, 10954–10967. [CrossRef] [PubMed]
68. Pal, N.; Banerjee, S.; Roy, P.; Pal, K. Melt-blending of unmodified and modified cellulose nanocrystals with reduced graphene oxide into PLA matrix for biomedical application. *Polym Advan Technol* **2019**, *30*, 3049–3060. [CrossRef]
69. Pal, N.; Banerjee, S.; Roy, P.; Pal, K. Reduced graphene oxide and PEG-grafted TEMPO-oxidized cellulose nanocrystal reinforced poly-lactic acid nanocomposite film for biomedical application. *Mater Sci Eng C Mater Biol Appl* **2019**, *104*, 109956. [CrossRef] [PubMed]
70. Song, N.; Cui, S.; Hou, X.; Ding, P.; Shi, L. Significant Enhancement of Thermal Conductivity in Nanofibrillated Cellulose Films with Low Mass Fraction of Nanodiamond. *ACS Appl Mater Interfaces* **2017**, *9*, 40766–40773. [CrossRef]
71. Ruiz-Palomero, C.; Benitez-Martinez, S.; Soriano, M.L.; Valcarcel, M. Fluorescent nanocellulosic hydrogels based on graphene quantum dots for sensing laccase. *Anal Chim Acta* **2017**, *974*, 93–99. [CrossRef] [PubMed]
72. Javanbakht, S.; Namazi, H. Doxorubicin loaded carboxymethyl cellulose/graphene quantum dot nanocomposite hydrogel films as a potential anticancer drug delivery system. *Mater Sci Eng C Mater Biol Appl* **2018**, *87*, 50–59. [CrossRef]
73. Anirudhan, T.S.; Deepa, J.R. Nano-zinc oxide incorporated graphene oxide/nanocellulose composite for the adsorption and photo catalytic degradation of ciprofloxacin hydrochloride from aqueous solutions. *J Colloid Interface Sci* **2017**, *490*, 343–356. [CrossRef]
74. Xu, Z.; Zhou, H.; Jiang, X.; Li, J.; Huang, F. Facile synthesis of reduced graphene oxide/trimethyl chlorosilane-coated cellulose nanofibres aerogel for oil absorption. *IET Nanobiotechnol* **2017**, *11*, 929–934. [CrossRef]
75. Yao, Q.; Fan, B.; Xiong, Y.; Jin, C.; Sun, Q.; Sheng, C. 3D assembly based on 2D structure of Cellulose Nanofibril/Graphene Oxide Hybrid Aerogel for Adsorptive Removal of Antibiotics in Water. *Sci Rep* **2017**, *7*, 45914. [CrossRef]
76. Alizadehgiashi, M.; Khuu, N.; Khabibullin, A.; Henry, A.; Tebbe, M.; Suzuki, T.; Kumacheva, E. Nanocolloidal Hydrogel for Heavy Metal Scavenging. *ACS Nano* **2018**, *12*, 8160–8168. [CrossRef] [PubMed]

77. Liang, Y.; Liu, J.; Wang, L.; Wan, Y.; Shen, J.; Bai, Q. Metal affinity-carboxymethyl cellulose functionalized magnetic graphene composite for highly selective isolation of histidine-rich proteins. *Talanta* **2019**, *195*, 381–389. [CrossRef] [PubMed]
78. Sun, H.X.; Ma, C.; Wang, T.; Xu, Y.Y.; Yuan, B.B.; Li, P.; Kong, Y. Preparation and Characterization of C60-Filled Ethyl Cellulose Mixed-Matrix Membranes for Gas Separation of Propylene/Propane. *Chem Eng Technol* **2014**, *37*, 611–619. [CrossRef]
79. Vetrivel, S.; Saraswathi, M.S.A.; Rana, D.; Nagendran, A. Fabrication of cellulose acetate nanocomposite membranes using 2D layered nanomaterials for macromolecular separation. *Int J Biol Macromol* **2018**, *107*, 1607–1612. [CrossRef] [PubMed]
80. Blomquist, N.; Wells, T.; Andres, B.; Backstrom, J.; Forsberg, S.; Olin, H. Metal-free supercapacitor with aqueous electrolyte and low-cost carbon materials. *Sci Rep* **2017**, *7*, 39836. [CrossRef]
81. Xu, X.; Hsieh, Y.L. Aqueous exfoliated graphene by amphiphilic nanocellulose and its application in moisture-responsive foldable actuators. *Nanoscale* **2019**, *11*, 11719–11729. [CrossRef]
82. Jiang, Q.; Tian, L.; Liu, K.K.; Tadepalli, S.; Raliya, R.; Biswas, P.; Naik, R.R.; Singamaneni, S. Bilayered Biofoam for Highly Efficient Solar Steam Generation. *Adv Mater* **2016**, *28*, 9400–9407. [CrossRef]
83. Li, X.; Shao, C.; Zhuo, B.; Yang, S.; Zhu, Z.; Su, C.; Yuan, Q. The use of nanofibrillated cellulose to fabricate a homogeneous and flexible graphene-based electric heating membrane. *Int J Biol Macromol* **2019**, *139*, 1103–1116. [CrossRef]
84. Kizling, M.; Draminska, S.; Stolarczyk, K.; Tammela, P.; Wang, Z.; Nyholm, L.; Bilewicz, R. Biosupercapacitors for powering oxygen sensing devices. *Bioelectrochemistry* **2015**, *106*, 34–40. [CrossRef]
85. Generalov, A.A.; Anoshkin, I.V.; Erdmanis, M.; Lioubtchenko, D.V.; Ovchinnikov, V.; Nasibulin, A.G.; Raisanen, A.V. Carbon nanotube network varactor. *Nanotechnology* **2015**, *26*, 045201. [CrossRef]
86. Asmat, S.; Husain, Q. Exquisite stability and catalytic performance of immobilized lipase on novel fabricated nanocellulose fused polypyrrole/graphene oxide nanocomposite: Characterization and application. *Int J Biol Macromol* **2018**, *117*, 331–341. [CrossRef] [PubMed]
87. Pal, N.; Dubey, P.; Gopinath, P.; Pal, K. Combined effect of cellulose nanocrystal and reduced graphene oxide into poly-lactic acid matrix nanocomposite as a scaffold and its anti-bacterial activity. *Int J Biol Macromol* **2017**, *95*, 94–105. [CrossRef] [PubMed]
88. Valentini, L.; Cardinali, M.; Fortunati, E.; Kenny, J.M. Nonvolatile memory behavior of nanocrystalline cellulose/graphene oxide composite films. *Appl Phys Lett* **2014**, *105*. [CrossRef]
89. Song, L.; Li, Y.; Xiong, Z.; Pan, L.; Luo, Q.; Xu, X.; Lu, S. Water-Induced shape memory effect of nanocellulose papers from sisal cellulose nanofibers with graphene oxide. *Carbohydr Polym* **2018**, *179*, 110–117. [CrossRef]
90. Wu, G.; Gu, Y.; Hou, X.; Li, R.; Ke, H.; Xiao, X. Hybrid Nanocomposites of Cellulose/Carbon-Nanotubes/Polyurethane with Rapidly Water Sensitive Shape Memory Effect and Strain Sensing Performance. *Polymers (Basel)* **2019**, *11*, 1586. [CrossRef] [PubMed]
91. Zhu, L.; Zhou, X.; Liu, Y.; Fu, Q. Highly Sensitive, Ultrastretchable Strain Sensors Prepared by Pumping Hybrid Fillers of Carbon Nanotubes/Cellulose Nanocrystal into Electrospun Polyurethane Membranes. *ACS Appl Mater Interfaces* **2019**, *11*, 12968–12977. [CrossRef]
92. Awan, F.; Bulger, E.; Berry, R.M.; Tam, K.C. Enhanced radical scavenging activity of polyhydroxylated C-60 functionalized cellulose nanocrystals. *Cellulose* **2016**, *23*, 3589–3599. [CrossRef]
93. Luo, J.; Deng, W.; Yang, F.; Wu, Z.; Huang, M.; Gu, M. Gold nanoparticles decorated graphene oxide/nanocellulose paper for NIR laser-induced photothermal ablation of pathogenic bacteria. *Carbohydr Polym* **2018**, *198*, 206–214. [CrossRef]
94. Anirudhan, T.S.; Sekhar, V.C.; Shainy, F.; Thomas, J.P. Effect of dual stimuli responsive dextran/nanocellulose polyelectrolyte complexes for chemophotothermal synergistic cancer therapy. *International Journal of Biological Macromolecules* **2019**, *135*, 776–789. [CrossRef]
95. Rasoulzadeh, M.; Namazi, H. Carboxymethyl cellulose/graphene oxide bio-nanocomposite hydrogel beads as anticancer drug carrier agent. *Carbohydr Polym* **2017**, *168*, 320–326. [CrossRef]
96. Wang, X.D.; Yu, K.X.; An, R.; Han, L.L.; Zhang, Y.L.; Shi, L.Y.; Ran, R. Self-assembling GO/modified HEC hybrid stabilized pickering emulsions and template polymerization for biomedical hydrogels. *Carbohyd Polym* **2019**, *207*, 694–703. [CrossRef] [PubMed]

97. Luo, X.; Zhang, H.; Cao, Z.; Cai, N.; Xue, Y.; Yu, F. A simple route to develop transparent doxorubicin-loaded nanodiamonds/cellulose nanocomposite membranes as potential wound dressings. *Carbohydr Polym* **2016**, *143*, 231–238. [CrossRef] [PubMed]
98. Anirudhan, T.S.; Deepa, J.R.; Binussreejayan. Electrochemical sensing of cholesterol by molecularly imprinted polymer of silylated graphene oxide and chemically modified nanocellulose polymer. *Mater Sci Eng C Mater Biol Appl* **2018**, *92*, 942–956. [CrossRef]
99. Fu, W.; Dai, Y.; Meng, X.; Xu, W.; Zhou, J.; Liu, Z.; Lu, W.; Wang, S.; Huang, C.; Sun, Y. Electronic textiles based on aligned electrospun belt-like cellulose acetate nanofibers and graphene sheets: portable, scalable and eco-friendly strain sensor. *Nanotechnology* **2019**, *30*, 045602. [CrossRef] [PubMed]
100. Zou, Y.; Zhang, Y.; Xu, Y.; Chen, Y.; Huang, S.; Lyu, Y.; Duan, H.; Chen, Z.; Tan, W. Portable and Label-Free Detection of Blood Bilirubin with Graphene-Isolated-Au-Nanocrystals Paper Strip. *Anal Chem* **2018**, *90*, 13687–13694. [CrossRef] [PubMed]
101. Jia, Y.; Yu, H.; Zhang, Y.; Dong, F.; Li, Z. Cellulose acetate nanofibers coated layer-by-layer with polyethylenimine and graphene oxide on a quartz crystal microbalance for use as a highly sensitive ammonia sensor. *Colloids Surf B Biointerfaces* **2016**, *148*, 263–269. [CrossRef] [PubMed]
102. Xue, T.; Sheng, Y.Y.; Xu, J.K.; Li, Y.Y.; Lu, X.Y.; Zhu, Y.F.; Duan, X.M.; Wen, Y.P. In-situ reduction of Ag+ on black phosphorene and its NH2-MWCNT nanohybrid with high stability and dispersibility as nanozyme sensor for three ATP metabolites. *Biosens Bioelectron* **2019**, *145*. [CrossRef]
103. Jung, M.; Kim, K.; Kim, B.; Lee, K.J.; Kang, J.W.; Jeon, S. Vertically stacked nanocellulose tactile sensor. *Nanoscale* **2017**, *9*, 17212–17219. [CrossRef]
104. Zhu, P.; Liu, Y.; Fang, Z.; Kuang, Y.; Zhang, Y.; Peng, C.; Chen, G. Flexible and Highly Sensitive Humidity Sensor Based on Cellulose Nanofibers and Carbon Nanotube Composite Film. *Langmuir* **2019**, *35*, 4834–4842. [CrossRef]
105. Chen, C.; Zhang, T.; Zhang, Q.; Chen, X.; Zhu, C.; Xu, Y.; Yang, J.; Liu, J.; Sun, D. Biointerface by Cell Growth on Graphene Oxide Doped Bacterial Cellulose/Poly(3,4-ethylenedioxythiophene) Nanofibers. *ACS Appl Mater Interfaces* **2016**, *8*, 10183–10192. [CrossRef]
106. Sun, Y.; Quan, Q.; Meng, H.; Zheng, Y.; Peng, J.; Hu, Y.; Feng, Z.; Sang, X.; Qiao, K.; He, W.; et al. Enhanced Neurite Outgrowth on a Multiblock Conductive Nerve Scaffold with Self-Powered Electrical Stimulation. *Adv Healthc Mater* **2019**, *8*, e1900127. [CrossRef] [PubMed]
107. Chakraborty, S.; Ponrasu, T.; Chandel, S.; Dixit, M.; Muthuvijayan, V. Reduced graphene oxide-loaded nanocomposite scaffolds for enhancing angiogenesis in tissue engineering applications. *R Soc Open Sci* **2018**, *5*, 172017. [CrossRef] [PubMed]
108. Chen, X.Y.; Low, H.R.; Loi, X.Y.; Merel, L.; Mohd Cairul Iqbal, M.A. Fabrication and evaluation of bacterial nanocellulose/poly(acrylic acid)/graphene oxide composite hydrogel: Characterizations and biocompatibility studies for wound dressing. *J Biomed Mater Res B Appl Biomater* **2019**, *107*, 2140–2151. [CrossRef] [PubMed]
109. Wang, Y.; Shi, L.; Wu, H.; Li, Q.; Hu, W.; Zhang, Z.; Huang, L.; Zhang, J.; Chen, D.; Deng, S.; et al. Graphene Oxide-IPDI-Ag/ZnO@Hydroxypropyl Cellulose Nanocomposite Films for Biological Wound-Dressing Applications. *ACS Omega* **2019**, *4*, 15373–15381. [CrossRef] [PubMed]
110. Burrs, S.L.; Bhargava, M.; Sidhu, R.; Kiernan-Lewis, J.; Gomes, C.; Claussen, J.C.; McLamore, E.S. A paper based graphene-nanocauliflower hybrid composite for point of care biosensing. *Biosens Bioelectron* **2016**, *85*, 479–487. [CrossRef] [PubMed]
111. Liu, C.; Dong, J.; Waterhouse, G.I.N.; Cheng, Z.Q.; Ai, S.Y. Electrochemical immunosensor with nanocellulose-Au composite assisted multiple signal amplification for detection of avian leukosis virus subgroup J. *Biosens Bioelectron* **2018**, *101*, 110–115. [CrossRef] [PubMed]
112. Cao, J.; Zhang, X.X.; Wu, X.D.; Wang, S.M.; Lu, C.H. Cellulose nanocrystals mediated assembly of graphene in rubber composites for chemical sensing applications. *Carbohyd Polym* **2016**, *140*, 88–95. [CrossRef]
113. Yan, C.Y.; Wang, J.X.; Kang, W.B.; Cui, M.Q.; Wang, X.; Foo, C.Y.; Chee, K.J.; Lee, P.S. Highly Stretchable Piezoresistive Graphene-Nanocellulose Nanopaper for Strain Sensors. *Advanced Materials* **2014**, *26*, 2022–2027. [CrossRef]
114. Wang, S.; Zhang, X.; Wu, X.; Lu, C. Tailoring percolating conductive networks of natural rubber composites for flexible strain sensors via a cellulose nanocrystal templated assembly. *Soft Matter* **2016**, *12*, 845–852. [CrossRef]

115. Baleizao, C.; Nagl, S.; Schaferling, M.; Berberan-Santos, M.N.; Wolfbeis, O.S. Dual fluorescence sensor for trace oxygen and temperature with unmatched range and sensitivity. *Anal Chem* **2008**, *80*, 6449–6457. [CrossRef]
116. Kochmann, S.; Baleizao, C.; Berberan-Santos, M.N.; Wolfbeis, O.S. Sensing and imaging of oxygen with parts per billion limits of detection and based on the quenching of the delayed fluorescence of (13)C70 fullerene in polymer hosts. *Anal Chem* **2013**, *85*, 1300–1304. [CrossRef] [PubMed]
117. Luo, Y.; Wang, S.; Shen, M.; Qi, R.; Fang, Y.; Guo, R.; Cai, H.; Cao, X.; Tomas, H.; Zhu, M.; et al. Carbon nanotube-incorporated multilayered cellulose acetate nanofibers for tissue engineering applications. *Carbohydr Polym* **2013**, *91*, 419–427. [CrossRef] [PubMed]
118. Duri, S.; Harkins, A.L.; Frazier, A.J.; Tran, C.D. Composites Containing Fullerenes and Polysaccharides: Green and Facile Synthesis, Biocompatibility, and Antimicrobial Activity. *Acs Sustain Chem Eng* **2017**, *5*, 5408–5417. [CrossRef]
119. Kopova, I.; Bacakova, L.; Lavrentiev, V.; Vacik, J. Growth and potential damage of human bone-derived cells on fresh and aged fullerene c60 films. *Int J Mol Sci* **2013**, *14*, 9182–9204. [CrossRef]
120. Kopova, I.; Lavrentiev, V.; Vacik, J.; Bacakova, L. Growth and potential damage of human bone-derived cells cultured on fresh and aged C60/Ti films. *PLoS One* **2015**, *10*, e0123680. [CrossRef]
121. Sheka, E.F. *Chapter 1: Concepts and grounds. In Fullerenes: Nanochemistry, Nanomagnetism, Nanomedicine, Nanophotonics*; Sheka, E.F., Ed.; CRC Press Taylor and Francis Group: Boca Raton, FL, USA, 2011; pp. 1–14. ISBN 9781439806425.
122. Sheka, E.F. Chapter 9: Nanomedicine of fullerene C60. In *Fullerenes: Nanochemistry, Nanomagnetism, Nanomedicine, Nanophotonics*, 1st ed.; Sheka, E.F., Ed.; CRC Press Taylor and Francis Group: Boca Raton, FL, USA, 2011; pp. 175–191. ISBN 9781439806425.
123. Li, J.; Kee, C.D.; Vadahanambi, S.; Oh, I.K. A Novel Biocompatible Actuator based on Electrospun Cellulose Acetate. *Adv Mater Res-Switz* **2011**, *214*, 359. [CrossRef]
124. Alekseeva, O.V.; Bagrovskaya, N.A.; Noskov, A.V. The Sorption Activity of a Cellulose-Fullerene Composite Relative to Heavy Metal Ions. *Prot Met Phys Chem+* **2019**, *55*, 15–20. [CrossRef]
125. Shams, S.S.; Zhang, R.Y.; Zhu, J. Graphene synthesis: a Review. *Mater Sci-Poland* **2015**, *33*, 566–578. [CrossRef]
126. Coros, M.; Pogacean, F.; Magerusan, L.; Socaci, C.; Pruneanu, S. A brief overview on synthesis and applications of graphene and graphene-based nanomaterials. *Front Mater Sci* **2019**, *13*, 23–32. [CrossRef]
127. Malho, J.M.; Laaksonen, P.; Walther, A.; Ikkala, O.; Linder, M.B. Facile Method for Stiff, Tough, and Strong Nanocomposites by Direct Exfoliation of Multilayered Graphene into Native Nanocellulose Matrix. *Biomacromolecules* **2012**, *13*, 1093–1099. [CrossRef]
128. Zhang, X.F.; Lu, Z.X.; Zhao, J.Q.; Li, Q.Y.; Zhang, W.; Lu, C.H. Exfoliation/dispersion of low-temperature expandable graphite in nanocellulose matrix by wet co-milling. *Carbohyd Polym* **2017**, *157*, 1434–1441. [CrossRef] [PubMed]
129. Zhang, G.Q.; Lv, J.L.; Yang, F.L. Optimized anti-biofouling performance of bactericides/cellulose nanocrystals composites modified PVDF ultrafiltration membrane for micro-polluted source water purification. *Water Sci Technol* **2019**, *79*, 1437–1446. [CrossRef]
130. Yuan, H.; Pan, H.; Meng, X.; Zhu, C.L.; Liu, S.Y.; Chen, Z.X.; Ma, J.; Zhu, S.M. Assembly of MnO/CNC/rGO fibers from colloidal liquid crystal for flexible supercapacitors via a continuous one-process method. *Nanotechnology* **2019**, *30*. [CrossRef]
131. Dhar, P.; Gaur, S.S.; Kumar, A.; Katiyar, V. Cellulose Nanocrystal Templated Graphene Nanoscrolls for High Performance Supercapacitors and Hydrogen Storage: An Experimental and Molecular Simulation Study. *Sci Rep-Uk* **2018**, *8*. [CrossRef]
132. Li, G.X.; Yu, J.Y.; Zhou, Z.Q.; Li, R.K.; Xiang, Z.H.; Cao, Q.; Zhao, L.L.; Peng, X.W.; Liu, H.; Zhou, W.J. N-Doped Mo2C Nanobelts/Graphene Nanosheets Bonded with Hydroxy Nanocellulose as Flexible and Editable Electrode for Hydrogen Evolution Reaction. *Iscience* **2019**, *19*, 1090. [CrossRef]
133. Zhou, X.M.; Liu, Y.; Du, C.Y.; Ren, Y.; Li, X.L.; Zuo, P.J.; Yin, G.P.; Ma, Y.L.; Cheng, X.Q.; Gao, Y.Z. Free-Standing Sandwich-Type Graphene/Nanocellulose/Silicon Laminar Anode for Flexible Rechargeable Lithium Ion Batteries. *Acs Appl Mater Inter* **2018**, *10*, 29638–29646. [CrossRef]
134. Wang, Z.H.; Tammela, P.; Stromme, M.; Nyholm, L. Nanocellulose coupled flexible polypyrrole@graphene oxide composite paper electrodes with high volumetric capacitance. *Nanoscale* **2015**, *7*, 3418–3423. [CrossRef]

135. Kumar, A.; Rao, K.M.; Han, S.S. Mechanically viscoelastic nanoreinforced hybrid hydrogels composed of polyacrylamide, sodium carboxymethylcellulose, graphene oxide, and cellulose nanocrystals. *Carbohyd Polym* **2018**, *193*, 228–238. [CrossRef]
136. Laaksonen, P.; Walther, A.; Malho, J.M.; Kainlauri, M.; Ikkala, O.; Linder, M.B. Genetic Engineering of Biomimetic Nanocomposites: Diblock Proteins, Graphene, and Nanofibrillated Cellulose. *Angew Chem Int Edit* **2011**, *50*, 8688–8691. [CrossRef]
137. Jia, L.L.; Huang, X.Y.; Liang, H.E.; Tao, Q. Enhanced hydrophilic and antibacterial efficiencies by the synergetic effect TiO2 nanofiber and graphene oxide in cellulose acetate nanofibers. *International Journal of Biological Macromolecules* **2019**, *132*, 1039–1043. [CrossRef]
138. Iijima, S. Helical Microtubules of Graphitic Carbon. *Nature* **1991**, *354*, 56–58. [CrossRef]
139. Stankova, L.; Fraczek-Szczypta, A.; Blazewicz, M.; Filova, E.; Blazewicz, S.; Lisa, V.; Bacakova, L. Human osteoblast-like MG 63 cells on polysulfone modified with carbon nanotubes or carbon nanohorns. *Carbon* **2014**, *67*, 578–591. [CrossRef]
140. Saito, T.; Kuramae, R.; Wohlert, J.; Berglund, L.A.; Isogai, A. An Ultrastrong Nanofibrillar Biomaterial: The Strength of Single Cellulose Nanofibrils Revealed via Sonication-Induced Fragmentation. *Biomacromolecules* **2013**, *14*, 248–253. [CrossRef]
141. Koga, H.; Saito, T.; Kitaoka, T.; Nogi, M.; Suganuma, K.; Isogai, A. Transparent, Conductive, and Printable Composites Consisting of TEMPO-Oxidized Nanocellulose and Carbon Nanotube. *Biomacromolecules* **2013**, *14*, 1160–1165. [CrossRef]
142. Fang, W.; Linder, M.B.; Laaksonen, P. Modification of carbon nanotubes by amphiphilic glycosylated proteins. *J Colloid Interf Sci* **2018**, *512*, 318–324. [CrossRef]
143. Mougel, J.B.; Bertoncini, P.; Cathala, B.; Chauvet, O.; Capron, I. Macroporous hybrid Pickering foams based on carbon nanotubes and cellulose nanocrystals. *J Colloid Interf Sci* **2019**, *544*, 78–87. [CrossRef]
144. Trigueiro, J.P.C.; Silva, G.G.; Pereira, F.V.; Lavall, R.L. Layer-by-layer assembled films of multi-walled carbon nanotubes with chitosan and cellulose nanocrystals. *J Colloid Interf Sci* **2014**, *432*, 214–220. [CrossRef]
145. Yang, X.; Shi, K.Y.; Zhitomirsky, I.; Cranston, E.D. Cellulose Nanocrystal Aerogels as Universal 3D Lightweight Substrates for Supercapacitor Materials. *Advanced Materials* **2015**, *27*, 6104–6109. [CrossRef]
146. ZabihiSahebi, A.; Koushkbaghi, S.; Pishnamazi, M.; Askari, A.; Khosravi, R.; Irani, M. Synthesis of cellulose acetate/chitosan/SWCNT/Fe3O4/TiO2 composite nanofibers for the removal of Cr(VI), As(V), Methylene blue and Congo red from aqueous solutions. *Int J Biol Macromol* **2019**, *140*, 1296–1304. [CrossRef]
147. Kang, Y.J.; Chun, S.J.; Lee, S.S.; Kim, B.Y.; Kim, J.H.; Chung, H.; Lee, S.Y.; Kim, W. All-solid-state flexible supercapacitors fabricated with bacterial nanocellulose papers, carbon nanotubes, and triblock-copolymer ion gels. *ACS Nano* **2012**, *6*, 6400–6406. [CrossRef]
148. Zhou, Y.; Lee, Y.; Sun, H.; Wallas, J.M.; George, S.M.; Xie, M. Coating Solution for High-Voltage Cathode: AlF3 Atomic Layer Deposition for Freestanding LiCoO2 Electrodes with High Energy Density and Excellent Flexibility. *ACS Appl Mater Interfaces* **2017**, *9*, 9614–9619. [CrossRef]
149. Gonzalez-Dominguez, J.M.; Anson-Casaos, A.; Grasa, L.; Abenia, L.; Salvador, A.; Colom, E.; Mesonero, J.E.; Garcia-Bordeje, J.E.; Benito, A.M.; Maser, W.K. Unique Properties and Behavior of Nonmercerized Type-II Cellulose Nanocrystals as Carbon Nanotube Biocompatible Dispersants. *Biomacromolecules* **2019**, *20*, 3147–3160. [CrossRef]
150. Zhang, H.; Sun, X.; Hubbe, M.A.; Pal, L. Highly conductive carbon nanotubes and flexible cellulose nanofibers composite membranes with semi-interpenetrating networks structure. *Carbohydr Polym* **2019**, *222*, 115013. [CrossRef]
151. Zhai, Y.; Wang, D.; Liu, H.; Zeng, Y.; Yin, Z.; Li, L. Electrochemical Molecular Imprinted Sensors Based on Electrospun Nanofiber and Determination of Ascorbic Acid. *Anal Sci* **2015**, *31*, 793–798. [CrossRef]
152. Broz, A.; Bacakova, L.; Stenclova, P.; Kromka, A.; Potocky, S. Uptake and intracellular accumulation of diamond nanoparticles - a metabolic and cytotoxic study. *Beilstein J Nanotechnol* **2017**, *8*, 1649–1657. [CrossRef]
153. Williams, O.A. Ultrananocrystalline diamond for electronic applications. *Semicond Sci Tech* **2006**, *21*, R49–R56. [CrossRef]
154. Shenderova, O.A.; Gruen, D.M. *Ultrananocrystalline Diamond: Synthesis, Properties and Applications of UNCD*, 2nd ed.; Shenderova, O.A., Gruen, D.M., Eds.; William Andrew Publishing: Oxford, UK, 2012; p. 584. ISBN 9781437734652.

155. Mochalin, V.N.; Shenderova, O.; Ho, D.; Gogotsi, Y. The properties and applications of nanodiamonds. *Nat Nanotechnol* **2011**, *7*, 11–23. [CrossRef]
156. Stankova, L.; Musilkova, J.; Broz, A.; Potocky, S.; Kromka, A.; Kozak, H.; Izak, T.; Artemenko, A.; Stranska, D.; Bacakova, L. Alterations to the adhesion, growth and osteogenic differentiation of human osteoblast-like cells on nanofibrous polylactide scaffolds with diamond nanoparticles. *Diam Relat Mater* **2019**, *97*. [CrossRef]
157. Grausova, L.; Kromka, A.; Burdikova, Z.; Eckhardt, A.; Rezek, B.; Vacik, J.; Haenen, K.; Lisa, V.; Bacakova, L. Enhanced Growth and Osteogenic Differentiation of Human Osteoblast-Like Cells on Boron-Doped Nanocrystalline Diamond Thin Films. *PLoS ONE* **2011**, *6*. [CrossRef]
158. Liskova, J.; Babchenko, O.; Varga, M.; Kromka, A.; Hadraba, D.; Svindrych, Z.; Burdikova, Z.; Bacakova, L. Osteogenic cell differentiation on H-terminated and O-terminated nanocrystalline diamond films. *Int J Nanomed* **2015**, *10*, 869–884. [CrossRef]
159. Morimune-Moriya, S.; Salajkova, M.; Zhou, Q.; Nishino, T.; Berglund, L.A. Reinforcement Effects from Nanodiamond in Cellulose Nanofibril Films. *Biomacromolecules* **2018**, *19*, 2423–2431. [CrossRef]
160. Juknius, T.; Ruzauskas, M.; Tamulevicius, T.; Siugzdiniene, R.; Jukniene, I.; Vasiliauskas, A.; Jurkeviciute, A.; Tamulevicius, S. Antimicrobial Properties of Diamond-Like Carbon/Silver Nanocomposite Thin Films Deposited on Textiles: Towards Smart Bandages. *Materials* **2016**, *9*, 371. [CrossRef]
161. Yuan, F.S.; Huang, Y.; Fan, M.M.; Chen, C.T.; Qian, J.S.; Hao, Q.L.; Yang, J.Z.; Sun, D.P. N-Doped Carbon Nanofibrous Network Derived from Bacterial Cellulose for the Loading of Pt Nanoparticles for Methanol Oxidation Reaction. *Chem-Eur J* **2018**, *24*, 1844–1852. [CrossRef]
162. Li, S.; Wang, M.Y.; Luo, Y.; Huang, J.G. Bio-Inspired Hierarchical Nanofibrous Fe3O4-TiO2-Carbon Composite as a High-Performance Anode Material for Lithium-Ion Batteries. *Acs Appl Mater Inter* **2016**, *8*, 17343–17351. [CrossRef]
163. Celik, K.B.; Cengiz, E.C.; Sar, T.; Dursun, B.; Ozturk, O.; Akbas, M.Y.; Demir-Cakan, R. In-situ wrapping of tin oxide nanoparticles by bacterial cellulose derived carbon nanofibers and its application as freestanding interlayer in lithium sulfide based lithium-sulfur batteries. *J Colloid Interf Sci* **2018**, *530*, 137–145. [CrossRef]
164. Xu, J.C.; Rong, J.; Qiu, F.X.; Zhu, Y.; Mao, K.L.; Fang, Y.Y.; Yang, D.Y.; Zhang, T. Highly dispersive NiCo2S4 nanoparticles anchored on nitrogen-doped carbon nanofibers for efficient hydrogen evolution reaction. *J Colloid Interf Sci* **2019**, *555*, 294–303. [CrossRef]
165. d'Amora, M.; Giordani, S. Carbon Nanomaterials for Nanomedicine. In *Micro and Nano Technologies*; Ciofani, G., Ed.; Elsevier: Amsterdam, The Netherlands, 2018; pp. 103–113. ISBN 978-0-12-814156-4. [CrossRef]
166. Chaudhuri, I.; Fruijtier-Polloth, C.; Ngiewih, Y.; Levy, L. Evaluating the evidence on genotoxicity and reproductive toxicity of carbon black: a critical review. *Crit Rev Toxicol* **2018**, *48*, 143–169. [CrossRef]
167. Niranjan, R.; Thakur, A.K. The Toxicological Mechanisms of Environmental Soot (Black Carbon) and Carbon Black: Focus on Oxidative Stress and Inflammatory Pathways. *Front Immunol* **2017**, *8*. [CrossRef]
168. Zhu, Y.; Li, W.X.; Zhang, Y.; Li, J.; Liang, L.; Zhang, X.Z.; Chen, N.; Sun, Y.H.; Chen, W.; Tai, R.Z.; et al. Excessive Sodium Ions Delivered into Cells by Nanodiamonds: Implications for Tumor Therapy. *Small* **2012**, *8*, 1771–1779. [CrossRef]
169. Kovacs, T.; Naish, V.; O'Connor, B.; Blaise, C.; Gagne, F.; Hall, L.; Trudeau, V.; Martel, P. An ecotoxicological characterization of nanocrystalline cellulose (NCC). *Nanotoxicology* **2010**, *4*, 255–270. [CrossRef]
170. Shvedova, A.A.; Kisin, E.R.; Yanamala, N.; Farcas, M.T.; Menas, A.L.; Williams, A.; Fournier, P.M.; Reynolds, J.S.; Gutkin, D.W.; Star, A.; et al. Gender differences in murine pulmonary responses elicited by cellulose nanocrystals. *Part Fibre Toxicol* **2016**, *13*. [CrossRef] [PubMed]
171. Sunasee, R.; Araoye, E.; Pyram, D.; Hemraz, U.D.; Boluk, Y.; Ckless, K. Cellulose nanocrystal cationic derivative induces NLRP3 inflammasome-dependent IL-1beta secretion associated with mitochondrial ROS production. *Biochem Biophys Rep* **2015**, *4*, 1–9. [CrossRef] [PubMed]
172. Ede, J.D.; Ong, K.J.; Goergen, M.; Rudie, A.; Pomeroy-Carter, C.A.; Shatkin, J.A. Risk Analysis of Cellulose Nanomaterials by Inhalation: Current State of Science. *Nanomaterials (Basel)* **2019**, *9*, 337. [CrossRef]
173. Przekora, A.; Vandrovcova, M.; Travnickova, M.; Pajorova, J.; Molitor, M.; Ginalska, G.; Bacakova, L. Evaluation of the potential of chitosan/beta-1,3-glucan/hydroxyapatite material as a scaffold for living bone graft production in vitro by comparison of ADSC and BMDSC behaviour on its surface. *Biomed Mater* **2017**, *12*, 015030. [CrossRef]

174. Bacakova, L.; Zarubova, J.; Travnickova, M.; Musilkova, J.; Pajorova, J.; Slepicka, P.; Kasalkova, N.S.; Svorcik, V.; Kolska, Z.; Motarjemi, H.; et al. Stem cells: their source, potency and use in regenerative therapies with focus on adipose-derived stem cells - a review. *Biotechnol Adv* **2018**, *36*, 1111–1126. [CrossRef] [PubMed]
175. Filova, E.; Bullett, N.A.; Bacakova, L.; Grausova, L.; Haycock, J.W.; Hlucilova, J.; Klima, J.; Shard, A. Regionally-selective cell colonization of micropatterned surfaces prepared by plasma polymerization of acrylic acid and 1,7-octadiene. *Physiol Res* **2009**, *58*, 669–684.